

Fairness-Aware Low-Rank Adaptation Under Demographic Privacy Constraints

Parameswaran Kamalaruban
Innovation Lab, Featurespace

kamal.parameswaran@featurespace.co.uk

Stuart Burrell
Innovation Lab, Featurespace

stuart.burrell@featurespace.co.uk

Piotr Skalski
Innovation Lab, Featurespace

piotr.skalski@featurespace.co.uk

Mark Anderson
Innovation Lab, Featurespace

mark.anderson@featurespace.co.uk

Maeve Madigan
Innovation Lab, Featurespace
maeve.madigan@featurespace.co.uk

David Sutton
Innovation Lab, Featurespace
david.sutton@featurespace.co.uk

Abstract

Pre-trained foundation models can be adapted for specific tasks using Low-Rank Adaptation (LoRA). However, the fairness properties of these adapted classifiers remain underexplored. Existing fairness-aware fine-tuning methods rely on direct access to sensitive attributes or their predictors, but in practice, these sensitive attributes are often held under strict consumer privacy controls, and neither the attributes nor their predictors are available to model developers, hampering the development of fair models. To address this issue, we introduce a set of LoRA-based fine-tuning methods that can be trained in a distributed fashion, where model developers and fairness auditors collaborate without sharing sensitive attributes or predictors. In this paper, we evaluate three such methods - sensitive unlearning, adversarial training, and orthogonality loss - against a fairness-unaware baseline, using experiments on the CelebA and UTK-Face datasets with an ImageNet pre-trained ViT-Base model. We find that orthogonality loss consistently reduces bias while maintaining or improving utility, whereas adversarial training improves False Positive Rate Parity and Demographic Parity in some cases, and sensitive unlearning provides no clear benefit. In tasks where significant biases are present, distributed fairness-aware fine-tuning methods can effectively eliminate bias without compromising consumer privacy and, in most cases, improve model utility.

1. Introduction

Pre-trained foundation models have catalyzed remarkable advances across domains such as computer vision and natural language processing [5, 49, 50]. Their ability to trans-

fer learning representations to various downstream tasks has led to widespread adoption. However, these models also inherit - and in some cases amplify - the biases present in their training data, potentially resulting in unfair or discriminatory downstream predictions [4, 8]. As models grow in size and are fine-tuned on specialized datasets to achieve peak performance, addressing these inherent biases becomes critical, particularly for sensitive applications in law, healthcare, or finance. Recent developments in parameter-efficient fine-tuning (PEFT) techniques [19], such as Low-Rank Adaptation (LoRA) [22], have enabled the efficient adaptation of massive pre-trained models by updating only a small number of additional parameters. Despite its computational benefits and modular design, the fairness implications of LoRA and related PEFT methods remain insufficiently understood.

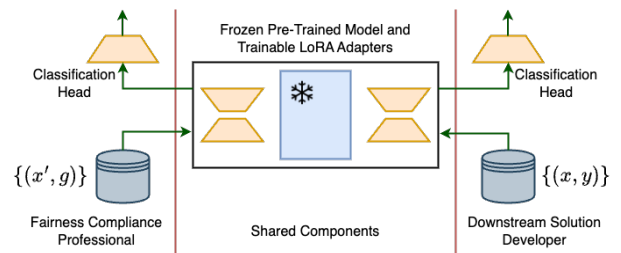


Figure 1. Collaborative debiasing of pre-trained foundation models under demographic privacy constraints.

In this work, we explore the use of LoRA adapters to mitigate bias for downstream model developers who lack access to sensitive attributes. In this setup, a pre-trained, frozen foundation model is shared between two distinct parties: the downstream solution developer (SD) and the fair-

ness compliance officer (CO). The SD possesses a dataset $\{(x, y)\}$, where x denotes input features and y represents the corresponding target labels, while the CO holds a separate dataset $\{(x', g)\}$, with x' drawn from a distribution similar to that of x and g denoting sensitive attributes. Our objective is to fine-tune the frozen foundation model such that the resulting downstream predictor not only maximizes task performance but also enforces fairness by making predictions invariant to the sensitive attribute g . To adhere to privacy and compliance constraints - particularly pertinent in domains like healthcare and finance where data sensitivity is paramount - neither party is permitted to share their raw data or the corresponding classification heads (i.e., the downstream and sensitive attribute prediction models). Instead, they are allowed to exchange only adapter modules that facilitate the joint fine-tuning process, thereby limiting the explicit transfer of sensitive information (see Figure 1). This federated learning-inspired setup mirrors real-world collaborative scenarios where stringent privacy regulations necessitate minimal inter-institutional data sharing.

Bias mitigation strategies in machine learning are broadly classified into pre-processing [9, 18, 25], in-processing [2, 3, 27, 45], and post-processing [20, 26, 33] approaches. In this work, we focus on in-processing methods that integrate fairness constraints directly into the fine-tuning stage of pre-trained models. Traditional fairness regularization techniques [3, 27], which typically require group labels to impose fairness penalties, are not applicable here due to the lack of shared sensitive annotations between the SD and the CO. Likewise, proxy sensitive attribute prediction methods [11, 51] - which necessitate the sharing of classification heads to infer bias - are infeasible under our stringent data-sharing constraints. Instead, our investigation leverages fair representation learning approaches that can be adapted to operate within our limited information sharing framework, decoupling sensitive attribute influences from learned representations while preserving the federated nature of the system.

Despite growing interest in the fairness implications of LoRA methods, most studies have focused on fairness-unaware LoRA fine-tuning. Recent work [13] evaluates subgroup fairness properties of LoRA fine-tuning but limits itself to standard downstream fine-tuning. Similarly, approaches like FairLoRA [34] and FairTune [15] integrate fairness objectives into fine-tuning but require direct access to sensitive labels. In contrast, our study leverages two separate datasets, (x, y) and (x', g) , to develop and evaluate fairness-aware LoRA-based strategies under strict privacy constraints.

Contributions. Our contributions are to:

1. Introduce a distributed fairness-aware fine-tuning framework for large pre-trained models that preserves con-

sumer privacy by decoupling sensitive attribute handling from model development. Our approach leverages LoRA to enable collaboration between model developers and fairness auditors without requiring the sharing of sensitive attributes or their predictors.

2. Adapt and evaluate three debiasing strategies within our framework:
 - *Sensitive Unlearning*: Repurpose an approach from language model detoxification [46] to mitigate bias in classification tasks.
 - *Adversarial Training*: Explore a well-established fairness method [1] in the context of LoRA fine-tuning.
 - *Orthogonality Loss*: Introduce an orthogonality constraint inspired by continual multi-task fine-tuning [39], where the sensitive adapter is used solely for regularization.

These are benchmarked against a fairness-unaware downstream fine-tuning baseline.

3. Demonstrate through extensive experiments on CelebA and UTK-Face - using an ImageNet pre-trained 86M ViT-Base model - that while sensitive unlearning and adversarial training yield moderate improvements, the adapted orthogonality loss method consistently reduces bias and often enhances overall utility.

2. Related Work

Algorithmic Fairness in Machine Learning. Algorithmic fairness is a rapidly evolving field focused on ensuring equitable outcomes in AI decision-making systems. Various approaches have been proposed to measure and mitigate biases within algorithms [6, 7, 37, 40]. Bias mitigation strategies are generally categorized into pre-processing, in-processing, and post-processing methods. Pre-processing methods modify the training data to reduce bias before model training [9, 18, 25], while post-processing techniques adjust model predictions to improve fairness after training [20, 26, 33]. In contrast, in-processing approaches incorporate fairness constraints directly into the learning objective and have been extensively studied in classical machine learning models [2, 3, 27, 45]. For a more comprehensive review of fairness and bias mitigation strategies in machine learning, we refer interested readers to recent surveys on the topic [10, 21, 32, 38].

Fairness-Aware Fine-Tuning. Recent studies have also explored fairness-aware fine-tuning in deep learning, particularly for pre-trained models. For instance, recent work [31] investigates last-layer fairness fine-tuning, where fairness constraints are introduced as regularization terms during the fine-tuning phase to mitigate bias in pre-trained deep neural networks. Methods such as FairLoRA [34] and FairTune [15] have been proposed to integrate fairness considerations directly into the fine-tuning process. FairLoRA aug-

ments the downstream classification loss with a fairness regularization term based on specific fairness metrics, whereas FairTune adopts a bi-level optimization framework where an inner loop performs standard downstream fine-tuning with masked LoRA modules and an outer loop adjusts these masks to optimize a fairness objective on a validation set. However, these approaches typically require direct access to sensitive labels and necessitate the sharing of classification heads, assumptions that are incompatible with privacy-preserving settings.

Merging of Adapters. Task Arithmetic [24] provides a simple mechanism for merging models by summing the task vectors derived from multiple tasks and applying the resultant vector to the pre-trained model. Recent research has further investigated the potential of arithmetic operations for merging adapters to facilitate efficient cross-task generalization and knowledge transfer. In particular, the study in [46] demonstrates that parameter-efficient modules can be composed through simple arithmetic operations, effectively merging task-specific knowledge while preserving modularity. Complementing these findings, LoraHub [23] explores dynamic composition strategies that enable seamless cross-task generalization by efficiently combining multiple LoRA adapters. Despite these promising developments, the process of merging LoRA adapters is not without challenges; catastrophic forgetting and knowledge conflicts can occur when integrating adapters trained on disparate tasks [35, 41, 42, 44]. Specifically, adding task vectors that point in largely opposite directions may lead to catastrophic forgetting, while inconsistent magnitudes among task vectors can result in unbalanced merging, ultimately undermining the effectiveness of the combined model.

3. Problem Setup and Background

Problem Setup. Following the limited information sharing framework described in Section 1, we consider a binary classification problem with a binary sensitive attribute. The downstream task dataset is denoted as $\mathcal{D}^{(\text{task})} = \{(x, y)\}$, where x represents the input features and $y \in \{0, 1\}$ is the target label. The sensitive task dataset is given by $\mathcal{D}^{(\text{sensitive})} = \{(x', g)\}$, with $g \in \{0, 1\}$ representing the sensitive attribute and the inputs drawn from a distribution similar to that of $\mathcal{D}^{(\text{task})}$. In our setting, a pre-trained, frozen foundation model is accessible to two parties: a downstream solution developer who holds $\mathcal{D}^{(\text{task})}$ and a fairness compliance professional who possesses $\mathcal{D}^{(\text{sensitive})}$. Our objective is to fine-tune the frozen model such that the resulting downstream predictor achieves high task performance while enforcing fairness by rendering its predictions invariant to the sensitive attribute g .

Utility and Fairness Metrics. We assess model performance using a comprehensive set of utility and group fairness metrics [12, 16, 20, 40]. Utility is measured through standard metrics such as accuracy (ACC), balanced accuracy (BA), precision (PPV), recall (TPR), false positive rate (FPR), F1-score (F1), as well as ROC-AUC and PR-AUC. In addition to these, we evaluate group fairness with respect to the binary sensitive attribute g (e.g., Male versus Female) by considering both difference and ratio metrics. For difference metrics, we compute the precision difference as $|\text{PPV}(\text{Male}) - \text{PPV}(\text{Female})|$, and the demographic parity difference as $|\mathbb{P}[\hat{Y} = 1 | G = \text{Male}] - \mathbb{P}[\hat{Y} = 1 | G = \text{Female}]|$. Similarly, ratio metrics are derived by taking the minimum of the ratios between groups for precision, and demographic parity (e.g., $\min\left\{\frac{\text{PPV}(\text{Male})}{\text{PPV}(\text{Female})}, \frac{\text{PPV}(\text{Female})}{\text{PPV}(\text{Male})}\right\}$). Ideal values for difference metrics are 0, with deviations above 0.1 often indicating bias, while ratio metrics ideally equal 1, with values below 0.9 signaling potential bias.

Low-Rank Adaptation. LoRA is a widely used PEFT method introduced by Hu et al. [22] that adapts pre-trained models by learning low-dimensional updates to the weight matrices. In LoRA, given a pre-trained weight matrix $W_0 \in \mathbb{R}^{d \times k}$, the model update is parameterized as a low-rank decomposition:

$$W = W_0 + \Delta W = W_0 + BA^\top,$$

where $A \in \mathbb{R}^{d \times r}$ and $B \in \mathbb{R}^{r \times k}$, with $\text{rank } r \ll \min(d, k)$. The matrices are initialized such that A is sampled from a Gaussian distribution, $A \sim \mathcal{N}(0, \sigma^2)$ for a small σ , and B is set to the zero matrix, ensuring that the initial update ΔW is zero and the pre-trained model’s behavior is preserved. During training, W_0 remains frozen, and only A and B are updated. For transformer-based architectures, LoRA adapters are typically applied to the query and value matrices of the self-attention layers, while an additional task-specific head is attached to the last layer for supervised learning. This approach significantly reduces the number of trainable parameters while maintaining competitive performance on downstream tasks.

4. Fairness-Aware Fine-Tuning

In this section, we present four fine-tuning strategies that leverage LoRA adapters to adapt a pre-trained model for binary classification in the limited information-sharing framework. We begin with the baseline fairness-unaware downstream fine-tuning approach (ERM), and then describe three fairness-aware methods - debias via sensitive unlearning (UNL), joint downstream and sensitive fine-tuning via adversarial training (ADV), and downstream fine-tuning augmented with an orthogonality loss (ORTH) - each designed

to mitigate the influence of sensitive attributes on model predictions while preserving task performance.

Fairness-unaware downstream fine-tuning (ERM). In this approach, the objective is to adapt the pre-trained model for the downstream task while keeping the base parameters frozen. Specifically, we train a downstream task adapter $\theta_{\text{ERM}}^{(\text{task})}$ along with its corresponding classification head $w_{\text{ERM}}^{(\text{task})}$ by minimizing the cross-entropy loss on the downstream dataset $\mathcal{D}^{(\text{task})}$ (see Figure 2). Formally, the training objective is defined as

$$\begin{aligned} (\theta_{\text{ERM}}^{(\text{task})}, w_{\text{ERM}}^{(\text{task})}) \leftarrow \arg \min_{\theta^{(\text{task})}, w^{(\text{task})}} & \left[\lambda_{\text{norm}} \cdot R_{\text{norm}}(\theta^{(\text{task})}) \right. \\ & \left. + \ell_{\text{CE}}(\theta^{(\text{pre})} \oplus \theta^{(\text{task})}, w^{(\text{task})}; \mathcal{D}^{(\text{task})}) \right], \quad (1) \end{aligned}$$

where $\theta^{(\text{pre})}$ denotes the pre-trained model, and \oplus represents the addition of the LoRA adapter with the pre-trained model. The norm regularization term [47] is defined as $R_{\text{norm}}(\theta^{(\text{task})}) = \sum_i \left[\|(A_i^{(\text{task})})^\top A_i^{(\text{task})} - I\|_F^2 + \|(B_i^{(\text{task})})^\top B_i^{(\text{task})} - I\|_F^2 \right]$, with $\theta^{(\text{task})} = \{(A_i^{(\text{task})}, B_i^{(\text{task})})\}$ representing the set of LoRA parameters, and λ_{norm} controlling the strength of the regularization.

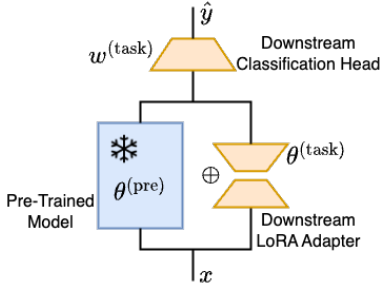


Figure 2. ERM: Fine-tune the pre-trained model for the downstream task.

Debias via sensitive unlearning followed by downstream fine-tuning (UNL). In this approach, we first isolate the sensitive attribute by fine-tuning a dedicated sensitive adapter. Specifically, we train a sensitive attribute adapter $\theta_{\text{ERM}}^{(\text{sen})}$ along with its classification head $w_{\text{ERM}}^{(\text{sen})}$ on the sensitive dataset $\mathcal{D}^{(\text{sen})}$ by minimizing the cross-entropy loss augmented with the norm regularization term. We solve

$$\begin{aligned} (\theta_{\text{ERM}}^{(\text{sen})}, w_{\text{ERM}}^{(\text{sen})}) \leftarrow \arg \min_{\theta^{(\text{sen})}, w^{(\text{sen})}} & \left[\lambda_{\text{norm}} \cdot R_{\text{norm}}(\theta^{(\text{sen})}) \right. \\ & \left. + \ell_{\text{CE}}(\theta^{(\text{pre})} \oplus \theta^{(\text{sen})}, w^{(\text{sen})}; \mathcal{D}^{(\text{sen})}) \right], \quad (2) \end{aligned}$$

with the pre-trained model $\theta^{(\text{pre})}$ remaining frozen. Once the sensitive attribute representation is learned, we de-bias

the pre-trained model by “unlearning” this capability; that is, we subtract a scaled version of the sensitive adapter’s contribution (denoted by the operator \ominus , which corresponds to negating either the LoRA-A or LoRA-B component) from the pre-trained weights. Subsequently, we train a downstream task adapter $\theta_{\text{UNL}}^{(\text{task})}$ and its classification head $w_{\text{UNL}}^{(\text{task})}$ on the downstream dataset $\mathcal{D}^{(\text{task})}$ (see Figure 3). The corresponding training objective becomes

$$\begin{aligned} (\theta_{\text{UNL}}^{(\text{task})}, w_{\text{UNL}}^{(\text{task})}) \leftarrow \arg \min_{\theta^{(\text{task})}, w^{(\text{task})}} & \left[\lambda_{\text{norm}} \cdot R_{\text{norm}}(\theta^{(\text{task})}) \right. \\ & \left. + \ell_{\text{CE}}(\theta^{(\text{pre})} \ominus \lambda_{\text{sen}} \cdot \theta_{\text{ERM}}^{(\text{sen})} \oplus \theta^{(\text{task})}, w^{(\text{task})}; \mathcal{D}^{(\text{task})}) \right], \quad (3) \end{aligned}$$

while keeping both $\theta^{(\text{pre})}$ and $\theta_{\text{ERM}}^{(\text{sen})}$ frozen. Here, λ_{sen} is a hyperparameter that controls the extent of unlearning.

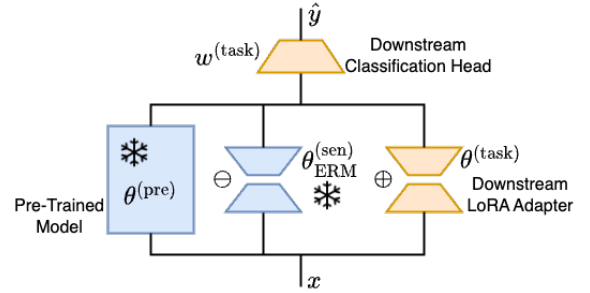


Figure 3. UNL: Fine-tune the pre-trained model for sensitive attribute prediction, debias it by “unlearning” this capability, and then perform downstream fine-tuning.

Joint downstream and sensitive fine-tuning via adversarial training (ADV). In this approach, we jointly fine-tune the downstream and sensitive adapters using an alternating optimization strategy. At each iteration k (where we perform several epochs over the dataset rather than a full minimization), we first update the sensitive adapter $\theta_k^{(\text{sen})}$ and its classification head $w_k^{(\text{sen})}$ by minimizing

$$\begin{aligned} (\theta_{k+1}^{(\text{sen})}, w_{k+1}^{(\text{sen})}) \leftarrow \arg \min_{\theta^{(\text{sen})}, w^{(\text{sen})}} & \left[\lambda_{\text{norm}} \cdot R_{\text{norm}}(\theta^{(\text{sen})}) + \right. \\ & \left. \ell_{\text{CE}}(\theta^{(\text{pre})} \oplus \theta^{(\text{sen})} \oplus \theta_k^{(\text{task})}, \text{GRL} \circ w^{(\text{sen})}; \mathcal{D}^{(\text{sen})}) \right], \quad (4) \end{aligned}$$

while keeping $\theta^{(\text{pre})}$ and $\theta_k^{(\text{task})}$ frozen, and initializing from $\theta_k^{(\text{sen})}$ and $w_k^{(\text{sen})}$. Here, the gradient reversal layer (GRL) is employed to maximize the loss with respect to the sensitive attribute. Once the sensitive adapter is updated, we fix it and update the downstream task adapter $\theta_k^{(\text{task})}$ and its

classification head $w_k^{(\text{task})}$ by minimizing

$$\begin{aligned} (\theta_{k+1}^{(\text{task})}, w_{k+1}^{(\text{task})}) \leftarrow \arg \min_{\theta^{(\text{task})}, w^{(\text{task})}} & \left[\lambda_{\text{norm}} \cdot R_{\text{norm}}(\theta^{(\text{task})}) \right. \\ & \left. + \ell_{\text{CE}}(\theta^{(\text{pre})} \oplus \theta_{k+1}^{(\text{sen})} \oplus \theta^{(\text{task})}, w^{(\text{task})}; \mathcal{D}^{(\text{task})}) \right], \quad (5) \end{aligned}$$

while keeping $\theta^{(\text{pre})}$ and $\theta_{k+1}^{(\text{sen})}$ frozen, and initializing from $\theta_k^{(\text{task})}$ and $w_k^{(\text{task})}$ (see Figure 4). This alternating optimization process is repeated until convergence, yielding the final adversarially trained adapters along with their classification heads: $(\theta_{\text{AT}}^{(\text{sen})}, w_{\text{AT}}^{(\text{sen})})$ and $(\theta_{\text{AT}}^{(\text{task})}, w_{\text{AT}}^{(\text{task})})$.

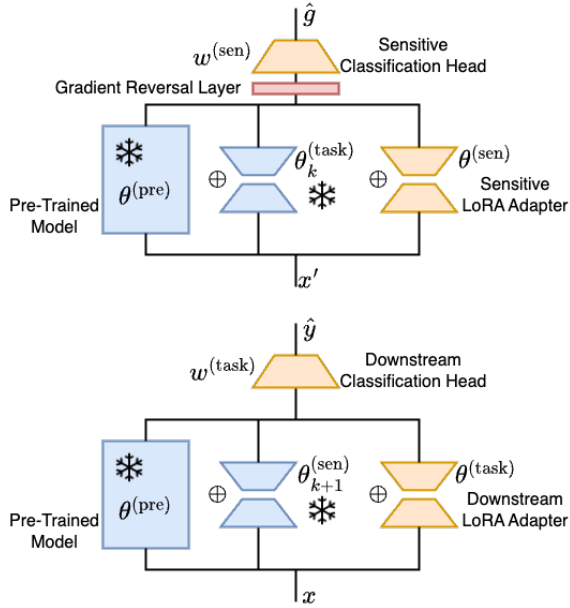


Figure 4. ADV: Jointly fine-tune for the downstream and sensitive tasks using an alternating optimization strategy that maximizes task performance while minimizing sensitive attribute predictability.

Downstream fine-tuning augmented with an orthogonality loss (ORTH). In this approach, we aim to enforce decorrelation between the learned representations for the sensitive attribute and those for the downstream task. First, a sensitive adapter $\theta_{\text{ERM}}^{(\text{sen})}$ along with its corresponding classification head $w_{\text{ERM}}^{(\text{sen})}$ is trained on the sensitive dataset $\mathcal{D}^{(\text{sen})}$ (see Eq. (2)). Subsequently, the downstream task adapter $\theta_{\text{ORTH}}^{(\text{task})}$ and its classification head $w_{\text{ORTH}}^{(\text{task})}$ are trained on the downstream dataset $\mathcal{D}^{(\text{task})}$ using a composite objective that combines the standard cross-entropy loss with an orthogonality regularization term designed to penalize correlations between the sensitive and downstream LoRA parameters.

The complete training objective is given by

$$\begin{aligned} (\theta_{\text{ORTH}}^{(\text{task})}, w_{\text{ORTH}}^{(\text{task})}) \leftarrow \arg \min_{\theta^{(\text{task})}, w^{(\text{task})}} & \left[\lambda_{\text{orth}} \cdot R_{\text{orth}}(\theta^{(\text{task})}, \theta_{\text{ERM}}^{(\text{sen})}) \right. \\ & + \lambda_{\text{norm}} \cdot R_{\text{norm}}(\theta^{(\text{task})}) \\ & \left. + \ell_{\text{CE}}(\theta^{(\text{pre})} \oplus \theta^{(\text{task})}, w^{(\text{task})}; \mathcal{D}^{(\text{task})}) \right], \quad (6) \end{aligned}$$

with both $\theta^{(\text{pre})}$ and $\theta_{\text{ERM}}^{(\text{sen})}$ held fixed. The orthogonality regularization term [17, 39] is defined as $R_{\text{orth}}(\theta^{(\text{task})}, \theta_{\text{ERM}}^{(\text{sen})}) = \sum_i \left[\|(A_i^{(\text{task})})^\top A_{\text{ERM},i}^{(\text{sen})} - I\|_F^2 + \|(B_i^{(\text{task})})^\top B_{\text{ERM},i}^{(\text{sen})} - I\|_F^2 \right]$, where $\theta^{(\text{task})} = \{(A_i^{(\text{task})}, B_i^{(\text{task})})\}$ and $\theta_{\text{ERM}}^{(\text{sen})} = \{(A_{\text{ERM},i}^{(\text{sen})}, B_{\text{ERM},i}^{(\text{sen})})\}$. The hyperparameter λ_{orth} controls the influence of the orthogonality constraint, thereby encouraging the downstream adapter to learn representations that are orthogonal to those associated with the sensitive attribute.

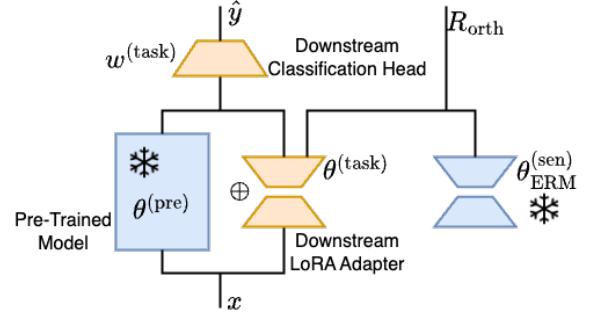


Figure 5. ORTH: Apply an orthogonality regularizer during downstream fine-tuning to enforce decorrelation between learned representations and sensitive features.

5. Experiments

In this section, we conduct a comprehensive evaluation of the fine-tuning strategies introduced in Section 4, assessing both utility and fairness performance. Specifically, we evaluate the ERM approach using the model $(\theta^{(\text{pre})} \oplus \theta_{\text{ERM}}^{(\text{task})}, w_{\text{ERM}}^{(\text{task})})$; the UNL approach using $(\theta^{(\text{pre})} \ominus \lambda_{\text{sen}} \cdot \theta_{\text{ERM}}^{(\text{sen})} \oplus \theta_{\text{UNL}}^{(\text{task})}, w_{\text{UNL}}^{(\text{task})})$; the ADV approach using $(\theta^{(\text{pre})} \oplus \theta_{\text{AT}}^{(\text{sen})} \oplus \theta_{\text{AT}}^{(\text{task})}, w_{\text{AT}}^{(\text{task})})$; and the ORTH approach using $(\theta^{(\text{pre})} \oplus \theta_{\text{ORTH}}^{(\text{task})}, w_{\text{ORTH}}^{(\text{task})})$.

5.1. Experimental Setup

Datasets. Our experiments are conducted on two widely used facial image datasets: UTK-Face [48] and CelebA [28]. UTK-Face contains 20,000 face images annotated with gender, age, and race information. For our study, we use age classification as the downstream task by partitioning the images into two groups (≤ 40 and > 40 years old) and designate gender as the sensitive attribute.

Table 1. Classifier threshold-dependent utility evaluation of fine-tuning strategies on UTK-Face and CelebA (gender as the sensitive attribute), averaged over three seeds.

	ACC (\uparrow)	BA (\uparrow)	PPV (\uparrow)	TPR (\uparrow)	FPR (\downarrow)	F1 (\uparrow)
UTK-Face (Age)						
ERM	0.897 \pm 0.003	0.895 \pm 0.003	0.800 \pm 0.007	0.891 \pm 0.003	0.100 \pm 0.002	0.843 \pm 0.005
UNL	0.891 \pm 0.003	0.888 \pm 0.002	0.789 \pm 0.009	0.881 \pm 0.001	0.104 \pm 0.004	0.832 \pm 0.005
ADV	0.872 \pm 0.007	0.866 \pm 0.006	0.761 \pm 0.019	0.851 \pm 0.007	0.118 \pm 0.011	0.803 \pm 0.011
ORTH	0.899 \pm 0.003	0.898 \pm 0.003	0.803 \pm 0.011	0.894 \pm 0.002	0.098 \pm 0.004	0.846 \pm 0.006
CelebA (Bald)						
ERM	0.983 \pm 0.001	0.962 \pm 0.002	0.575 \pm 0.013	0.940 \pm 0.005	0.016 \pm 0.001	0.713 \pm 0.010
UNL	0.983 \pm 0.000	0.956 \pm 0.001	0.569 \pm 0.008	0.927 \pm 0.002	0.016 \pm 0.000	0.705 \pm 0.006
ADV	0.950 \pm 0.005	0.962 \pm 0.002	0.304 \pm 0.020	0.975 \pm 0.007	0.050 \pm 0.005	0.462 \pm 0.023
ORTH	0.986 \pm 0.000	0.984 \pm 0.001	0.605 \pm 0.012	0.983 \pm 0.002	0.014 \pm 0.000	0.749 \pm 0.009
CelebA (Smiling)						
ERM	0.930 \pm 0.001	0.930 \pm 0.001	0.932 \pm 0.003	0.922 \pm 0.001	0.062 \pm 0.003	0.927 \pm 0.001
UNL	0.929 \pm 0.001	0.928 \pm 0.001	0.936 \pm 0.002	0.914 \pm 0.004	0.057 \pm 0.003	0.925 \pm 0.001
ADV	0.901 \pm 0.006	0.901 \pm 0.007	0.911 \pm 0.004	0.881 \pm 0.013	0.080 \pm 0.004	0.896 \pm 0.007
ORTH	0.932 \pm 0.001	0.932 \pm 0.001	0.938 \pm 0.002	0.920 \pm 0.002	0.057 \pm 0.002	0.929 \pm 0.001
CelebA (Wearing Hat)						
ERM	0.985 \pm 0.001	0.980 \pm 0.001	0.778 \pm 0.010	0.974 \pm 0.004	0.014 \pm 0.001	0.865 \pm 0.005
UNL	0.985 \pm 0.001	0.977 \pm 0.002	0.771 \pm 0.019	0.968 \pm 0.004	0.014 \pm 0.001	0.858 \pm 0.010
ADV	0.972 \pm 0.001	0.970 \pm 0.004	0.635 \pm 0.009	0.967 \pm 0.006	0.028 \pm 0.001	0.767 \pm 0.008
ORTH	0.986 \pm 0.000	0.988 \pm 0.001	0.786 \pm 0.003	0.990 \pm 0.002	0.014 \pm 0.000	0.876 \pm 0.003

Table 2. Classifier threshold-dependent fairness difference evaluation of fine-tuning strategies on UTK-Face and CelebA (gender as the sensitive attribute), averaged over three seeds. Bias intensity is color-coded from green (lowest) to orange-red (highest). Ideal fairness difference values are 0, with values exceeding 0.1 often indicating bias.

	Δ ACC (\downarrow)	Δ BA (\downarrow)	Δ PPV (\downarrow)	Δ TPR (\downarrow)	Δ FPR (\downarrow)	Δ F1 (\downarrow)	DP (\downarrow)
UTK-Face (Age)							
ERM	0.042 \pm 0.007	0.011 \pm 0.004	0.011 \pm 0.002	0.070 \pm 0.006	0.087 \pm 0.007	0.026 \pm 0.004	0.204 \pm 0.009
UNL	0.035 \pm 0.007	0.009 \pm 0.001	0.015 \pm 0.011	0.086 \pm 0.010	0.082 \pm 0.010	0.047 \pm 0.007	0.209 \pm 0.011
ADV	0.034 \pm 0.007	0.004 \pm 0.004	0.060 \pm 0.018	0.057 \pm 0.013	0.064 \pm 0.015	0.059 \pm 0.009	0.181 \pm 0.008
ORTH	0.040 \pm 0.004	0.007 \pm 0.003	0.013 \pm 0.007	0.076 \pm 0.004	0.088 \pm 0.004	0.027 \pm 0.001	0.207 \pm 0.008
CelebA (Bald)							
ERM	0.039 \pm 0.001	0.209 \pm 0.078	0.293 \pm 0.078	0.433 \pm 0.181	0.038 \pm 0.002	0.355 \pm 0.101	0.086 \pm 0.002
UNL	0.040 \pm 0.001	0.195 \pm 0.001	0.349 \pm 0.057	0.429 \pm 0.003	0.038 \pm 0.001	0.411 \pm 0.058	0.084 \pm 0.000
ADV	0.079 \pm 0.005	0.054 \pm 0.002	0.341 \pm 0.016	0.025 \pm 0.007	0.083 \pm 0.005	0.496 \pm 0.016	0.128 \pm 0.005
ORTH	0.034 \pm 0.001	0.026 \pm 0.000	0.194 \pm 0.090	0.017 \pm 0.002	0.035 \pm 0.001	0.177 \pm 0.081	0.085 \pm 0.000
CelebA (Smiling)							
ERM	0.013 \pm 0.002	0.018 \pm 0.001	0.036 \pm 0.001	0.042 \pm 0.003	0.006 \pm 0.001	0.039 \pm 0.002	0.146 \pm 0.002
UNL	0.016 \pm 0.001	0.023 \pm 0.002	0.038 \pm 0.002	0.048 \pm 0.002	0.002 \pm 0.001	0.043 \pm 0.002	0.144 \pm 0.002
ADV	0.021 \pm 0.003	0.027 \pm 0.002	0.077 \pm 0.011	0.032 \pm 0.013	0.023 \pm 0.011	0.054 \pm 0.003	0.116 \pm 0.010
ORTH	0.014 \pm 0.001	0.020 \pm 0.001	0.036 \pm 0.001	0.042 \pm 0.002	0.003 \pm 0.001	0.039 \pm 0.001	0.145 \pm 0.002
CelebA (Wearing Hat)							
ERM	0.007 \pm 0.001	0.010 \pm 0.003	0.132 \pm 0.004	0.028 \pm 0.006	0.009 \pm 0.001	0.094 \pm 0.004	0.066 \pm 0.002
UNL	0.009 \pm 0.001	0.004 \pm 0.001	0.129 \pm 0.010	0.009 \pm 0.007	0.009 \pm 0.001	0.085 \pm 0.010	0.064 \pm 0.001
ADV	0.012 \pm 0.003	0.006 \pm 0.002	0.203 \pm 0.021	0.013 \pm 0.004	0.012 \pm 0.002	0.156 \pm 0.017	0.066 \pm 0.002
ORTH	0.006 \pm 0.001	0.002 \pm 0.001	0.134 \pm 0.007	0.012 \pm 0.002	0.008 \pm 0.001	0.090 \pm 0.004	0.065 \pm 0.002

Table 3. Classifier threshold-dependent fairness ratio evaluation of fine-tuning strategies on UTK-Face and CelebA (gender as the sensitive attribute), averaged over three seeds. Bias intensity is color-coded from **green** (lowest) to **orange-red** (highest). Ideal fairness ratio values are 1, with values below 0.9 often indicating bias.

	ACC (\uparrow)	BA (\uparrow)	PPV (\uparrow)	TPR (\uparrow)	FPR (\uparrow)	F1 (\uparrow)	DP (\uparrow)
UTK-Face (Age)							
ERM	0.955 \pm 0.008	0.988 \pm 0.004	0.986 \pm 0.002	0.924 \pm 0.006	0.407 \pm 0.022	0.970 \pm 0.004	0.539 \pm 0.019
UNL	0.961 \pm 0.008	0.990 \pm 0.001	0.981 \pm 0.013	0.906 \pm 0.011	0.451 \pm 0.040	0.945 \pm 0.008	0.529 \pm 0.019
ADV	0.962 \pm 0.008	0.995 \pm 0.004	0.924 \pm 0.022	0.935 \pm 0.015	0.595 \pm 0.061	0.929 \pm 0.011	0.580 \pm 0.011
ORTH	0.956 \pm 0.005	0.992 \pm 0.003	0.984 \pm 0.008	0.918 \pm 0.004	0.395 \pm 0.002	0.968 \pm 0.002	0.534 \pm 0.015
CelebA (Bald)							
ERM	0.961 \pm 0.001	0.782 \pm 0.083	0.495 \pm 0.127	0.544 \pm 0.193	0.007 \pm 0.002	0.503 \pm 0.139	0.004 \pm 0.001
UNL	0.960 \pm 0.001	0.793 \pm 0.001	0.387 \pm 0.108	0.538 \pm 0.002	0.008 \pm 0.003	0.418 \pm 0.086	0.005 \pm 0.001
ADV	0.920 \pm 0.005	0.946 \pm 0.002	0.027 \pm 0.009	0.975 \pm 0.007	0.168 \pm 0.013	0.036 \pm 0.012	0.116 \pm 0.012
ORTH	0.966 \pm 0.001	0.974 \pm 0.000	0.685 \pm 0.146	0.983 \pm 0.002	0.008 \pm 0.002	0.766 \pm 0.107	0.005 \pm 0.001
CelebA (Smiling)							
ERM	0.986 \pm 0.002	0.981 \pm 0.001	0.962 \pm 0.001	0.955 \pm 0.004	0.915 \pm 0.010	0.958 \pm 0.002	0.727 \pm 0.003
UNL	0.982 \pm 0.001	0.975 \pm 0.002	0.960 \pm 0.002	0.949 \pm 0.002	0.975 \pm 0.021	0.954 \pm 0.002	0.728 \pm 0.003
ADV	0.977 \pm 0.003	0.970 \pm 0.002	0.918 \pm 0.012	0.964 \pm 0.015	0.766 \pm 0.111	0.940 \pm 0.004	0.774 \pm 0.020
ORTH	0.985 \pm 0.001	0.979 \pm 0.001	0.962 \pm 0.002	0.955 \pm 0.002	0.952 \pm 0.013	0.959 \pm 0.001	0.727 \pm 0.004
CelebA (Wearing Hat)							
ERM	0.992 \pm 0.001	0.990 \pm 0.003	0.839 \pm 0.004	0.971 \pm 0.006	0.567 \pm 0.026	0.895 \pm 0.005	0.346 \pm 0.008
UNL	0.991 \pm 0.001	0.996 \pm 0.001	0.841 \pm 0.015	0.991 \pm 0.007	0.548 \pm 0.006	0.903 \pm 0.012	0.345 \pm 0.002
ADV	0.988 \pm 0.003	0.994 \pm 0.002	0.715 \pm 0.027	0.987 \pm 0.004	0.653 \pm 0.049	0.810 \pm 0.019	0.407 \pm 0.009
ORTH	0.994 \pm 0.001	0.998 \pm 0.001	0.839 \pm 0.007	0.988 \pm 0.002	0.595 \pm 0.037	0.900 \pm 0.004	0.352 \pm 0.011

In contrast, CelebA comprises 202,599 face images with 40 binary attribute annotations; here, we consider several binary prediction tasks (e.g., smiling versus not smiling) as downstream tasks while again treating gender as the sensitive attribute. All images from both datasets are resized to 224×224 to match the input dimensions of our base model and are normalized prior to processing. We randomly split each dataset into training (70%), validation (15%), and test (15%) sets.

Base Model. For our base model, we employ an ImageNet pre-trained Vision Transformer (ViT-Base) [14], specifically the `vit-base-patch16-224-in21k` version with 86.6M parameters, which is obtained from Huggingface¹. This model was pre-trained on ImageNet-21k, comprising 14 million images across 21,843 classes, at a resolution of 224×224 .

Training Details. We employ a class-balancing sampling strategy and optimize the models using the AdamW optimizer [29] with a batch size of 256, a learning rate of 0.0001, and a weight decay of 0.0005. Training runs for 5 epochs with a CosineAnnealingLR scheduler, where $T_{\max} = 5$. For the LoRA adapters, we set the rank to 4,

¹<https://huggingface.co/google/vit-base-patch16-224-in21k>

the alpha parameter to 8, and apply a dropout rate of 0.1. Our implementation utilizes the PEFT library from Hugging Face [30].

5.2. Results

Our experiments evaluate the performance of the fine-tuning strategies discussed in Section 4 using both utility and fairness metrics, as implemented in the Fairlearn package [40]. All results are averaged over three random seeds for robustness and are reported on the UTK-Face and CelebA datasets, using a classifier threshold of 0.5 - except for the threshold-independent evaluation in Table 4.

Table 1 summarizes overall utility performance. The ORTH approach consistently achieves slightly higher utility compared to the other methods, while the ADV approach exhibits marginally lower performance, likely due to the trade-offs inherent in its alternating min-max optimization. Fairness evaluations based on difference metrics are shown in Table 2. For most tasks, significant bias (difference values exceeding 0.1) is absent; however, in the bald prediction task, the ERM baseline shows notable disparities in metrics such as BA, PPV, TPR, and F1 differences, which the ORTH approach substantially mitigates.

Table 3 presents fairness results based on ratio metrics. Here, significant bias - quantified as ratio values below 0.9 - is more apparent w.r.t. FPR and DP ratio metrics, likely

Table 4. Classifier threshold-independent utility and fairness evaluation of fine-tuning strategies on UTK-Face and CelebA (gender as the sensitive attribute), averaged over three seeds. Bias intensity is color-coded from **green** (lowest) to **orange-red** (highest). Ideal difference values are 0 (values above 0.1 indicating bias), while ideal ratio values are 1 (values below 0.9 indicating bias).

	ROC (\uparrow)	PR (\uparrow)	Δ ROC (\downarrow)	Δ PR (\downarrow)	ROC ratio (\uparrow)	PR ratio (\uparrow)
UTK-Face (Age)						
ERM	0.964 \pm 0.002	0.934 \pm 0.005	0.004 \pm 0.002	0.027 \pm 0.002	0.996 \pm 0.002	0.971 \pm 0.002
UNL	0.958 \pm 0.001	0.925 \pm 0.003	0.002 \pm 0.000	0.042 \pm 0.001	0.998 \pm 0.000	0.955 \pm 0.001
ADV	0.941 \pm 0.003	0.898 \pm 0.006	0.005 \pm 0.000	0.062 \pm 0.007	0.995 \pm 0.000	0.932 \pm 0.007
ORTH	0.966 \pm 0.001	0.937 \pm 0.004	0.004 \pm 0.001	0.025 \pm 0.003	0.996 \pm 0.001	0.973 \pm 0.003
CelebA (Bald)						
ERM	0.995 \pm 0.000	0.819 \pm 0.002	0.008 \pm 0.003	0.341 \pm 0.082	0.992 \pm 0.003	0.596 \pm 0.114
UNL	0.994 \pm 0.001	0.822 \pm 0.009	0.007 \pm 0.003	0.365 \pm 0.043	0.993 \pm 0.003	0.557 \pm 0.055
ADV	0.991 \pm 0.001	0.728 \pm 0.021	0.016 \pm 0.002	0.455 \pm 0.122	0.983 \pm 0.002	0.378 \pm 0.179
ORTH	0.997 \pm 0.000	0.850 \pm 0.004	0.008 \pm 0.000	0.138 \pm 0.049	0.992 \pm 0.000	0.846 \pm 0.060
CelebA (Smiling)						
ERM	0.983 \pm 0.000	0.983 \pm 0.001	0.008 \pm 0.000	0.018 \pm 0.000	0.992 \pm 0.000	0.982 \pm 0.000
UNL	0.982 \pm 0.000	0.983 \pm 0.000	0.009 \pm 0.000	0.019 \pm 0.000	0.991 \pm 0.000	0.980 \pm 0.000
ADV	0.966 \pm 0.004	0.968 \pm 0.004	0.016 \pm 0.001	0.034 \pm 0.003	0.983 \pm 0.001	0.965 \pm 0.003
ORTH	0.984 \pm 0.001	0.984 \pm 0.001	0.008 \pm 0.000	0.017 \pm 0.000	0.992 \pm 0.000	0.982 \pm 0.000
CelebA (Wearing Hat)						
ERM	0.998 \pm 0.000	0.966 \pm 0.001	0.001 \pm 0.000	0.043 \pm 0.003	0.999 \pm 0.000	0.956 \pm 0.003
UNL	0.997 \pm 0.000	0.956 \pm 0.004	0.001 \pm 0.001	0.035 \pm 0.003	0.999 \pm 0.001	0.963 \pm 0.003
ADV	0.994 \pm 0.001	0.918 \pm 0.006	0.002 \pm 0.001	0.074 \pm 0.008	0.998 \pm 0.001	0.922 \pm 0.009
ORTH	0.999 \pm 0.000	0.973 \pm 0.002	0.000 \pm 0.000	0.033 \pm 0.001	1.000 \pm 0.000	0.966 \pm 0.001

due to class imbalance in the downstream tasks. The ADV approach shows some reduction in bias for these metrics, though not significantly. As in the difference metrics, the bald prediction task highlights significant disparities in the ERM approach that are notably reduced by ORTH.

Table 4 offers a comprehensive, classifier threshold-independent evaluation using AUC-based metrics that capture both utility and fairness. This evaluation confirms that the ORTH method consistently outperforms the other strategies across all dimensions. For most tasks, significant bias - defined as a difference above 0.1 or a ratio below 0.9 - is minimal; yet, in the bald prediction task, the ORTH method considerably improves bias, as evidenced by enhanced PR AUC differences and ratio values.

Collectively, these findings indicate that the ORTH fine-tuning strategy not only maintains high downstream performance but also significantly reduces bias in scenarios where the ERM baseline exhibits considerable disparities. In contrast, the ADV and UNL methods offer limited benefits over ERM. When using threshold-dependent fairness metrics, ORTH consistently reduces bias, while ADV shows improvements in FPR and DP ratios for some tasks. Overall, these results underscore the promise of the ORTH approach as a fairness-aware fine-tuning strategy under demographic privacy constraints.

6. Conclusion

This work presents a distributed framework for fairness-aware fine-tuning that leverages LoRA to separate sensitive attribute handling from model development, thereby preserving consumer privacy while facilitating collaboration between model developers and fairness auditors. We adapt three debiasing strategies - sensitive unlearning, adversarial training, and orthogonality loss - and benchmark them against a fairness-unaware baseline. Experiments on the CelebA and UTK-Face datasets demonstrate that, while sensitive unlearning and adversarial training yield moderate improvements, the orthogonality loss method consistently reduces bias and often enhances overall utility.

These promising findings open several avenues for future investigation. Potential directions include exploring combinations of the debiasing strategies (e.g., integrating adversarial training with orthogonality loss) and refining classifier threshold tuning to better balance utility and fairness within the limited information sharing setup. Additionally, investigating differentially private methods for sharing LoRA adapters may further enhance privacy, though such approaches could pose challenges in maintaining the effectiveness of bias mitigation and utility [36, 43].

References

- [1] Tameem Adel, Isabel Valera, Zoubin Ghahramani, and Adrian Weller. One-Network Adversarial Fairness. In *AAAI*, 2019. 2
- [2] Alekh Agarwal, Alina Beygelzimer, Miroslav Dudík, John Langford, and Hanna Wallach. A Reductions Approach to Fair Classification. In *ICML*, 2018. 2
- [3] Alekh Agarwal, Miroslav Dudík, and Zhiwei Steven Wu. Fair Regression: Quantitative Definitions and Reduction-based Algorithms. In *ICML*, 2019. 2
- [4] Junaid Ali, Matthäus Kleindessner, Florian Wenzel, Kailash Budhathoki, Volkan Cevher, and Chris Russell. Evaluating the Fairness of Discriminative Foundation Models in Computer Vision. In *AIES*, 2023. 1
- [5] Muhammad Awais, Muzammal Naseer, Salman Khan, Rao Muhammad Anwer, Hisham Cholakkal, Mubarak Shah, Ming-Hsuan Yang, and Fahad Shahbaz Khan. Foundation Models Defining a New Era in Vision: a Survey and Outlook. *IEEE TPAMI*, 2025. 1
- [6] Solon Barocas, Moritz Hardt, and Arvind Narayanan. *Fairness and Machine Learning: Limitations and Opportunities*. MIT press, 2023. 2
- [7] Rachel KE Bellamy et al. AI Fairness 360: An Extensible Toolkit for Detecting and Mitigating Algorithmic Bias. *IBM Journal of Research and Development*, 2019. 2
- [8] Rishi Bommasani, Drew A Hudson, Ehsan Adeli, Russ Altman, Simran Arora, Sydney von Arx, Michael S Bernstein, Jeannette Bohg, Antoine Bosselut, Emma Brunskill, et al. On the Opportunities and Risks of Foundation Models. *arXiv preprint arXiv:2108.07258*, 2021. 1
- [9] Flavio Calmon, Dennis Wei, Bhanukiran Vinzamuri, Karthikeyan Natesan Ramamurthy, and Kush R Varshney. Optimized Pre-Processing for Discrimination Prevention. *NeurIPS*, 2017. 2
- [10] Simon Caton and Christian Haas. Fairness in Machine Learning: A Survey. *ACM Comput. Surv.*, 2024. 2
- [11] Jiahao Chen, Nathan Kallus, Xiaojie Mao, Geoffrey Svacha, and Madeleine Udell. Fairness Under Unawareness: Assessing Disparity When Protected Class Is Unobserved. In *ACM FAccT*, 2019. 2
- [12] Alexandra Chouldechova. Fair Prediction with Disparate Impact: A Study of Bias in Recidivism Prediction Instruments. *Big data*, 2017. 3
- [13] Zhoujie Ding, Ken Ziyu Liu, Pura Peetathawatchai, Berivan Isik, and Sanmi Koyejo. On Fairness of Low-Rank Adaptation of Large Models. *arXiv preprint arXiv:2405.17512*, 2024. 2
- [14] Alexey Dosovitskiy et al. An Image is Worth 16x16 Words: Transformers for Image Recognition at Scale. In *ICLR*, 2021. 7
- [15] Raman Dutt, Ondrej Bohdal, Sotirios A Tsaftaris, and Timothy Hospedales. FairTune: Optimizing Parameter Efficient Fine Tuning for Fairness in Medical Image Analysis. In *ICLR*, 2024. 2
- [16] Cynthia Dwork, Moritz Hardt, Toniann Pitassi, Omer Reingold, and Richard Zemel. Fairness Through Awareness. In *Proceedings of the Innovations in Theoretical Computer Science Conference*, 2012. 3
- [17] Mehrdad Farajtabar, Navid Azizan, Alex Mott, and Ang Li. Orthogonal Gradient Descent for Continual Learning. In *AISTATS*, 2020. 5
- [18] Michael Feldman, Sorelle A Friedler, John Moeller, Carlos Scheidegger, and Suresh Venkatasubramanian. Certifying and Removing Disparate Impact. In *KDD*, 2015. 2
- [19] Zeyu Han, Chao Gao, Jinyang Liu, Jeff Zhang, and Sai Qian Zhang. Parameter-Efficient Fine-Tuning for Large Models: A Comprehensive Survey. *arXiv preprint arXiv:2403.14608*, 2024. 1
- [20] Moritz Hardt, Eric Price, and Nati Srebro. Equality of Opportunity in Supervised Learning. *NeurIPS*, 2016. 2, 3
- [21] Max Hort, Zhenpeng Chen, Jie M Zhang, Mark Harman, and Federica Sarro. Bias Mitigation for Machine Learning Classifiers: A Comprehensive Survey. *ACM Journal on Responsible Computing*, 2024. 2
- [22] Edward J Hu, Phillip Wallis, Zeyuan Allen-Zhu, Yuanzhi Li, Shean Wang, Lu Wang, Weizhu Chen, et al. LoRA: Low-Rank Adaptation of Large Language Models. In *ICLR*, 2022. 1, 3
- [23] Chengsong Huang, Qian Liu, Bill Yuchen Lin, Tianyu Pang, Chao Du, and Min Lin. LoraHub: Efficient Cross-Task Generalization via Dynamic LoRA Composition. In *COLM*, 2024. 3
- [24] Gabriel Ilharco, Marco Tulio Ribeiro, Mitchell Wortsman, Ludwig Schmidt, Hannaneh Hajishirzi, and Ali Farhadi. Editing Models with Task Arithmetic. In *ICLR*, 2023. 3
- [25] Faisal Kamiran and Toon Calders. Data Pre-Processing Techniques for Classification without Discrimination. *Knowledge and Information Systems*, 2012. 2
- [26] Faisal Kamiran, Asim Karim, and Xiangliang Zhang. Decision Theory for Discrimination-Aware Classification. In *ICDM*, 2012. 2
- [27] Toshihiro Kamishima, Shotaro Akaho, Hideki Asoh, and Jun Sakuma. Fairness-Aware Classifier with Prejudice Remover Regularizer. In *ECML PKDD*, 2012. 2
- [28] Ziwei Liu, Ping Luo, Xiaogang Wang, and Xiaoou Tang. Deep Learning Face Attributes in the Wild. In *ICCV*, 2015. 5
- [29] Ilya Loshchilov and Frank Hutter. Decoupled Weight Decay Regularization. In *ICLR*, 2024. 7
- [30] Sourab Mangrulkar, Sylvain Gugger, Lysandre Debut, Younes Belkada, Sayak Paul, and Benjamin Bossan. PEFT: State-of-the-art Parameter-Efficient Fine-Tuning methods, 2022. 7
- [31] Yuzhen Mao, Zhun Deng, Huaxiu Yao, Ting Ye, Kenji Kawaguchi, and James Zou. Last-Layer Fairness Fine-tuning is Simple and Effective for Neural Networks. *arXiv preprint arXiv:2304.03935*, 2023. 2
- [32] Ninareh Mehrabi, Fred Morstatter, Nripsuta Saxena, Kristina Lerman, and Aram Galstyan. A Survey on Bias and Fairness in Machine Learning. *ACM computing surveys (CSUR)*, 2021. 2
- [33] Geoff Pleiss, Manish Raghavan, Felix Wu, Jon Kleinberg, and Kilian Q Weinberger. On Fairness and Calibration. *NeurIPS*, 2017. 2

- [34] Rohan Sukumaran, Aarash Feizi, Adriana Romero-Sorian, and Golnoosh Farnadi. FairLoRA: Unpacking Bias Mitigation in Vision Models with Fairness-Driven Low-Rank Adaptation. *arXiv preprint arXiv:2410.17358*, 2024. 2
- [35] Wenju Sun, Qingyong Li, Wen Wang, Yangli-ao Geng, and Boyang Li. Task Arithmetic in Trust Region: A Training-Free Model Merging Approach to Navigate Knowledge Conflicts. *arXiv preprint arXiv:2501.15065*, 2025. 3
- [36] Youbang Sun, Zitao Li, Yaliang Li, and Bolin Ding. Improving LoRA in Privacy-Preserving Federated Learning. In *ICLR*, 2024. 8
- [37] Sahil Verma and Julia Rubin. Fairness Definitions Explained. In *Proceedings of the International Workshop on Software Fairness*, 2018. 2
- [38] Mingyang Wan, Daochen Zha, Ninghao Liu, and Na Zou. In-Processing Modeling Techniques for Machine Learning Fairness: A Survey. *ACM Transactions on Knowledge Discovery from Data*, 2023. 2
- [39] Xiao Wang, Tianze Chen, Qiming Ge, Han Xia, Rong Bao, Rui Zheng, Qi Zhang, Tao Gui, and Xuanjing Huang. Orthogonal Subspace Learning for Language Model Continual Learning. In *EMNLP*, 2023. 2, 5
- [40] Hilde Weerts, Miroslav Dudík, Richard Edgar, Adrin Jalali, Roman Lutz, and Michael Madaio. Fairlearn: Assessing and Improving Fairness of AI Systems. *JMLR*, 2023. 2, 3, 7
- [41] Prateek Yadav, Derek Tam, Leshem Choshen, Colin A Raffel, and Mohit Bansal. TIES-Merging: Resolving Interference When Merging Models. *NeurIPS*, 2023. 3
- [42] Enneng Yang, Zhenyi Wang, Li Shen, Shiwei Liu, Guibing Guo, Xingwei Wang, and Dacheng Tao. AdaMerging: Adaptive Model Merging for Multi-Task Learning. In *ICLR*, 2024. 3
- [43] Da Yu et al. Differentially Private Fine-tuning of Language Models. In *ICLR*, 2022. 8
- [44] Le Yu, Bowen Yu, Haiyang Yu, Fei Huang, and Yongbin Li. Language Models are Super Mario: Absorbing Abilities from Homologous Models as a Free Lunch. In *ICML*, 2024. 3
- [45] Brian Hu Zhang, Blake Lemoine, and Margaret Mitchell. Mitigating Unwanted Biases with Adversarial Learning. In *AIES*, 2018. 2
- [46] Jinghan Zhang, Shiqi Chen, Junteng Liu, and Junxian He. Composing Parameter-Efficient Modules with Arithmetic Operations. *NeurIPS*, 2023. 2, 3
- [47] Qingru Zhang, Minshuo Chen, Alexander Bukharin, Pengcheng He, Yu Cheng, Weizhu Chen, and Tuo Zhao. Adaptive Budget Allocation for Parameter-Efficient Fine-Tuning. In *ICLR*, 2023. 4
- [48] Zhifei Zhang, Yang Song, and Hairong Qi. Age Progression/Regression by Conditional Adversarial Autoencoder. In *CVPR*, 2017. 5
- [49] Wayne Xin Zhao et al. A Survey of Large Language Models. *arXiv preprint arXiv:2303.18223*, 2023. 1
- [50] Ce Zhou et al. A Comprehensive Survey on Pretrained Foundation Models: A History from BERT to ChatGPT. *International Journal of Machine Learning and Cybernetics*, 2024. 1
- [51] Zhaowei Zhu, Yuanshun Yao, Jiankai Sun, Hang Li, and Yang Liu. Weak Proxies are Sufficient and Preferable for Fairness with Missing Sensitive Attributes. In *ICML*, 2023. 2

Fairness-Aware Low-Rank Adaptation Under Demographic Privacy Constraints

Supplementary Material

A. Additional Results

Tables 5-8 report utility and fairness results for additional downstream tasks on the CelebA dataset. The trends observed in the tabulated results are also visually captured in the radar charts (see Figures 6-14), which provide a quick, intuitive overview of the trade-offs between utility and fairness.

Table 5. Classifier threshold-dependent utility evaluation of fine-tuning strategies on UTK-Face and CelebA (gender as the sensitive attribute), averaged over three seeds.

	ACC (\uparrow)	BA (\uparrow)	PPV (\uparrow)	TPR (\uparrow)	FPR (\downarrow)	F1 (\uparrow)
CelebA (Black Hair)						
ERM	0.890 \pm 0.001	0.902 \pm 0.001	0.703 \pm 0.005	0.925 \pm 0.003	0.121 \pm 0.002	0.799 \pm 0.003
UNL	0.889 \pm 0.001	0.899 \pm 0.000	0.706 \pm 0.004	0.917 \pm 0.001	0.119 \pm 0.002	0.798 \pm 0.002
ADV	0.858 \pm 0.002	0.871 \pm 0.003	0.645 \pm 0.004	0.897 \pm 0.008	0.154 \pm 0.004	0.750 \pm 0.003
ORTH	0.894 \pm 0.001	0.905 \pm 0.001	0.713 \pm 0.003	0.925 \pm 0.003	0.115 \pm 0.001	0.805 \pm 0.002
CelebA (Eyeglasses)						
ERM	0.995 \pm 0.000	0.990 \pm 0.001	0.937 \pm 0.003	0.985 \pm 0.002	0.005 \pm 0.000	0.960 \pm 0.002
UNL	0.995 \pm 0.000	0.989 \pm 0.002	0.937 \pm 0.001	0.982 \pm 0.004	0.005 \pm 0.000	0.959 \pm 0.001
ADV	0.988 \pm 0.002	0.985 \pm 0.001	0.860 \pm 0.016	0.982 \pm 0.001	0.011 \pm 0.002	0.917 \pm 0.009
ORTH	0.995 \pm 0.000	0.994 \pm 0.001	0.940 \pm 0.002	0.993 \pm 0.002	0.004 \pm 0.000	0.966 \pm 0.001
CelebA (Young)						
ERM	0.866 \pm 0.001	0.865 \pm 0.001	0.956 \pm 0.001	0.866 \pm 0.001	0.136 \pm 0.004	0.909 \pm 0.001
UNL	0.867 \pm 0.003	0.864 \pm 0.002	0.955 \pm 0.001	0.869 \pm 0.004	0.141 \pm 0.004	0.910 \pm 0.002
ADV	0.735 \pm 0.069	0.745 \pm 0.055	0.909 \pm 0.021	0.727 \pm 0.082	0.237 \pm 0.031	0.805 \pm 0.060
ORTH	0.870 \pm 0.001	0.870 \pm 0.002	0.957 \pm 0.002	0.871 \pm 0.004	0.131 \pm 0.007	0.912 \pm 0.001
CelebA (Attractive)						
ERM	0.829 \pm 0.000	0.829 \pm 0.000	0.836 \pm 0.002	0.828 \pm 0.002	0.169 \pm 0.002	0.832 \pm 0.001
UNL	0.826 \pm 0.000	0.826 \pm 0.001	0.827 \pm 0.002	0.834 \pm 0.003	0.183 \pm 0.004	0.831 \pm 0.001
ADV	0.740 \pm 0.044	0.739 \pm 0.045	0.739 \pm 0.045	0.767 \pm 0.029	0.289 \pm 0.060	0.752 \pm 0.038
ORTH	0.831 \pm 0.001	0.831 \pm 0.001	0.832 \pm 0.003	0.837 \pm 0.001	0.176 \pm 0.002	0.835 \pm 0.001
CelebA (Blond Hair)						
ERM	0.937 \pm 0.001	0.945 \pm 0.001	0.714 \pm 0.003	0.958 \pm 0.002	0.067 \pm 0.001	0.818 \pm 0.002
UNL	0.938 \pm 0.002	0.944 \pm 0.002	0.716 \pm 0.006	0.953 \pm 0.002	0.065 \pm 0.002	0.818 \pm 0.004
ADV	0.914 \pm 0.002	0.916 \pm 0.001	0.645 \pm 0.007	0.919 \pm 0.006	0.087 \pm 0.004	0.758 \pm 0.003
ORTH	0.939 \pm 0.001	0.948 \pm 0.001	0.722 \pm 0.003	0.962 \pm 0.002	0.065 \pm 0.001	0.825 \pm 0.001

Table 6. Classifier threshold-dependent fairness difference evaluation of fine-tuning strategies on UTK-Face and CelebA (gender as the sensitive attribute), averaged over three seeds. Bias intensity is color-coded from **green** (lowest) to **orange-red** (highest). Ideal fairness difference values are 0, with values exceeding 0.1 often indicating bias.

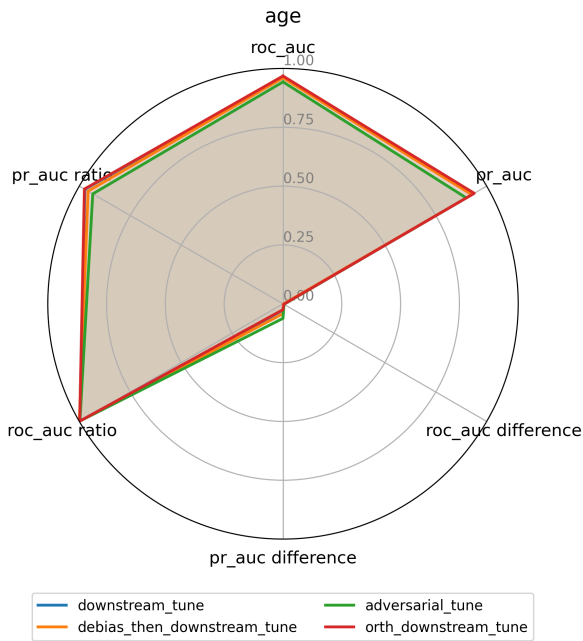
	$\Delta_{\text{ACC}} (\downarrow)$	$\Delta_{\text{BA}} (\downarrow)$	$\Delta_{\text{PPV}} (\downarrow)$	$\Delta_{\text{TPR}} (\downarrow)$	$\Delta_{\text{FPR}} (\downarrow)$	$\Delta_{\text{F1}} (\downarrow)$	DP (\downarrow)
CelebA (Black Hair)							
ERM	0.043 \pm 0.001	0.028 \pm 0.002	0.006 \pm 0.002	0.011 \pm 0.005	0.067 \pm 0.002	0.007 \pm 0.001	0.133 \pm 0.002
UNL	0.046 \pm 0.001	0.030 \pm 0.001	0.006 \pm 0.002	0.008 \pm 0.002	0.069 \pm 0.001	0.002 \pm 0.001	0.129 \pm 0.001
ADV	0.048 \pm 0.002	0.047 \pm 0.003	0.024 \pm 0.006	0.033 \pm 0.009	0.060 \pm 0.007	0.004 \pm 0.002	0.108 \pm 0.007
ORTH	0.040 \pm 0.002	0.026 \pm 0.001	0.010 \pm 0.004	0.012 \pm 0.006	0.063 \pm 0.004	0.008 \pm 0.002	0.130 \pm 0.003
CelebA (Eyeglasses)							
ERM	0.008 \pm 0.001	0.006 \pm 0.001	0.011 \pm 0.005	0.005 \pm 0.002	0.007 \pm 0.001	0.006 \pm 0.001	0.106 \pm 0.003
UNL	0.008 \pm 0.000	0.007 \pm 0.000	0.016 \pm 0.007	0.007 \pm 0.000	0.007 \pm 0.000	0.008 \pm 0.001	0.103 \pm 0.002
ADV	0.015 \pm 0.002	0.013 \pm 0.002	0.051 \pm 0.013	0.011 \pm 0.003	0.015 \pm 0.002	0.025 \pm 0.007	0.110 \pm 0.004
ORTH	0.007 \pm 0.000	0.004 \pm 0.001	0.010 \pm 0.005	0.003 \pm 0.001	0.007 \pm 0.000	0.006 \pm 0.002	0.106 \pm 0.003
CelebA (Young)							
ERM	0.080 \pm 0.004	0.015 \pm 0.003	0.036 \pm 0.001	0.145 \pm 0.007	0.115 \pm 0.004	0.097 \pm 0.003	0.303 \pm 0.005
UNL	0.085 \pm 0.002	0.012 \pm 0.003	0.036 \pm 0.001	0.151 \pm 0.003	0.128 \pm 0.002	0.101 \pm 0.002	0.311 \pm 0.003
ADV	0.135 \pm 0.010	0.025 \pm 0.007	0.087 \pm 0.042	0.269 \pm 0.005	0.239 \pm 0.037	0.205 \pm 0.023	0.361 \pm 0.035
ORTH	0.080 \pm 0.004	0.014 \pm 0.005	0.033 \pm 0.000	0.145 \pm 0.005	0.116 \pm 0.008	0.096 \pm 0.003	0.305 \pm 0.002
CelebA (Attractive)							
ERM	0.013 \pm 0.001	0.018 \pm 0.004	0.113 \pm 0.004	0.264 \pm 0.012	0.228 \pm 0.006	0.194 \pm 0.005	0.469 \pm 0.005
UNL	0.013 \pm 0.002	0.008 \pm 0.004	0.114 \pm 0.002	0.258 \pm 0.004	0.242 \pm 0.004	0.189 \pm 0.002	0.469 \pm 0.002
ADV	0.016 \pm 0.008	0.013 \pm 0.005	0.238 \pm 0.064	0.265 \pm 0.054	0.240 \pm 0.044	0.260 \pm 0.014	0.402 \pm 0.074
ORTH	0.013 \pm 0.002	0.009 \pm 0.002	0.118 \pm 0.003	0.248 \pm 0.007	0.229 \pm 0.002	0.185 \pm 0.004	0.465 \pm 0.001
CelebA (Blond Hair)							
ERM	0.061 \pm 0.001	0.042 \pm 0.008	0.332 \pm 0.002	0.167 \pm 0.015	0.082 \pm 0.002	0.297 \pm 0.001	0.274 \pm 0.003
UNL	0.058 \pm 0.001	0.069 \pm 0.000	0.345 \pm 0.009	0.216 \pm 0.001	0.079 \pm 0.001	0.320 \pm 0.007	0.268 \pm 0.001
ADV	0.033 \pm 0.004	0.056 \pm 0.003	0.523 \pm 0.004	0.157 \pm 0.006	0.045 \pm 0.002	0.493 \pm 0.007	0.224 \pm 0.002
ORTH	0.058 \pm 0.000	0.039 \pm 0.001	0.326 \pm 0.001	0.158 \pm 0.003	0.080 \pm 0.001	0.289 \pm 0.002	0.272 \pm 0.002

Table 7. Classifier threshold-dependent fairness ratio evaluation of fine-tuning strategies on UTK-Face and CelebA (gender as the sensitive attribute), averaged over three seeds. Bias intensity is color-coded from **green** (lowest) to **orange-red** (highest). Ideal fairness ratio values are 1, with values below 0.9 often indicating bias.

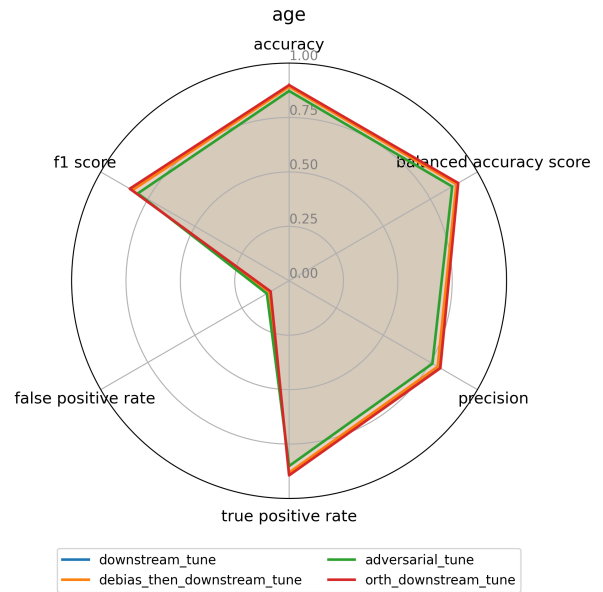
	ACC (\uparrow)	BA (\uparrow)	PPV (\uparrow)	TPR (\uparrow)	FPR (\uparrow)	F1 (\uparrow)	DP (\uparrow)
CelebA (Black Hair)							
ERM	0.953 \pm 0.001	0.969 \pm 0.002	0.992 \pm 0.002	0.988 \pm 0.006	0.584 \pm 0.010	0.992 \pm 0.001	0.658 \pm 0.005
UNL	0.950 \pm 0.001	0.967 \pm 0.001	0.992 \pm 0.003	0.991 \pm 0.002	0.574 \pm 0.008	0.997 \pm 0.001	0.664 \pm 0.004
ADV	0.945 \pm 0.003	0.947 \pm 0.003	0.964 \pm 0.008	0.963 \pm 0.010	0.686 \pm 0.023	0.994 \pm 0.002	0.727 \pm 0.012
ORTH	0.956 \pm 0.002	0.972 \pm 0.001	0.987 \pm 0.006	0.988 \pm 0.006	0.591 \pm 0.021	0.990 \pm 0.003	0.660 \pm 0.008
CelebA (Eyeglasses)							
ERM	0.992 \pm 0.001	0.994 \pm 0.001	0.989 \pm 0.005	0.995 \pm 0.002	0.200 \pm 0.017	0.994 \pm 0.001	0.190 \pm 0.005
UNL	0.992 \pm 0.000	0.993 \pm 0.000	0.983 \pm 0.007	0.993 \pm 0.000	0.217 \pm 0.019	0.992 \pm 0.001	0.194 \pm 0.008
ADV	0.985 \pm 0.002	0.987 \pm 0.002	0.941 \pm 0.016	0.989 \pm 0.003	0.257 \pm 0.034	0.972 \pm 0.008	0.204 \pm 0.014
ORTH	0.993 \pm 0.000	0.996 \pm 0.001	0.989 \pm 0.006	0.997 \pm 0.001	0.201 \pm 0.017	0.994 \pm 0.002	0.189 \pm 0.005
CelebA (Young)							
ERM	0.911 \pm 0.005	0.982 \pm 0.004	0.963 \pm 0.001	0.841 \pm 0.007	0.461 \pm 0.009	0.896 \pm 0.004	0.633 \pm 0.005
UNL	0.906 \pm 0.002	0.986 \pm 0.003	0.962 \pm 0.001	0.836 \pm 0.003	0.439 \pm 0.004	0.893 \pm 0.002	0.627 \pm 0.004
ADV	0.828 \pm 0.005	0.963 \pm 0.013	0.906 \pm 0.047	0.664 \pm 0.033	0.398 \pm 0.082	0.759 \pm 0.043	0.530 \pm 0.003
ORTH	0.912 \pm 0.004	0.983 \pm 0.006	0.966 \pm 0.001	0.842 \pm 0.005	0.446 \pm 0.008	0.898 \pm 0.003	0.632 \pm 0.002
CelebA (Attractive)							
ERM	0.985 \pm 0.001	0.977 \pm 0.005	0.868 \pm 0.005	0.703 \pm 0.013	0.265 \pm 0.009	0.778 \pm 0.006	0.331 \pm 0.007
UNL	0.984 \pm 0.002	0.990 \pm 0.005	0.866 \pm 0.003	0.711 \pm 0.005	0.269 \pm 0.006	0.783 \pm 0.002	0.340 \pm 0.004
ADV	0.977 \pm 0.013	0.983 \pm 0.007	0.697 \pm 0.090	0.684 \pm 0.052	0.428 \pm 0.131	0.678 \pm 0.029	0.430 \pm 0.095
ORTH	0.985 \pm 0.002	0.988 \pm 0.003	0.862 \pm 0.004	0.723 \pm 0.007	0.277 \pm 0.003	0.788 \pm 0.005	0.342 \pm 0.002
CelebA (Blond Hair)							
ERM	0.938 \pm 0.001	0.955 \pm 0.008	0.553 \pm 0.004	0.828 \pm 0.015	0.229 \pm 0.004	0.646 \pm 0.001	0.129 \pm 0.002
UNL	0.940 \pm 0.001	0.926 \pm 0.000	0.536 \pm 0.010	0.776 \pm 0.001	0.231 \pm 0.009	0.619 \pm 0.008	0.126 \pm 0.006
ADV	0.965 \pm 0.004	0.938 \pm 0.004	0.280 \pm 0.008	0.831 \pm 0.006	0.586 \pm 0.029	0.395 \pm 0.009	0.258 \pm 0.015
ORTH	0.940 \pm 0.000	0.958 \pm 0.001	0.564 \pm 0.003	0.838 \pm 0.003	0.229 \pm 0.003	0.658 \pm 0.003	0.128 \pm 0.002

Table 8. Classifier threshold-independent utility and fairness evaluation of fine-tuning strategies on UTK-Face and CelebA (gender as the sensitive attribute), averaged over three seeds. Bias intensity is color-coded from **green** (lowest) to **orange-red** (highest). Ideal difference values are 0 (values above 0.1 indicating bias), while ideal ratio values are 1 (values below 0.9 indicating bias).

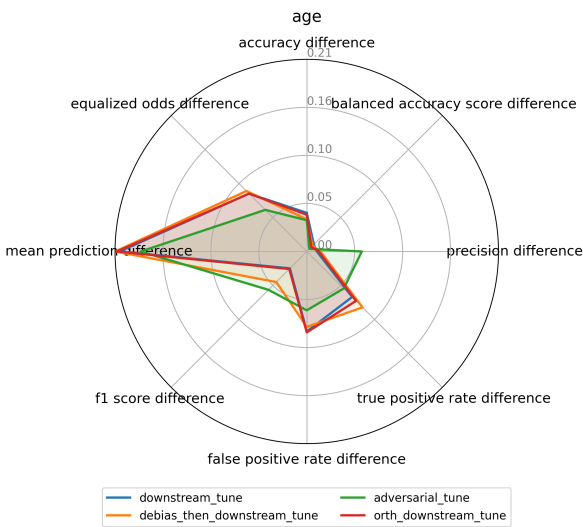
	ROC (\uparrow)	PR (\uparrow)	Δ ROC (\downarrow)	Δ PR (\downarrow)	ROC ratio (\uparrow)	PR ratio (\uparrow)
CelebA (Black Hair)						
ERM	0.966 \pm 0.001	0.895 \pm 0.001	0.015 \pm 0.000	0.017 \pm 0.002	0.985 \pm 0.001	0.982 \pm 0.003
UNL	0.964 \pm 0.000	0.892 \pm 0.000	0.018 \pm 0.001	0.008 \pm 0.002	0.982 \pm 0.001	0.991 \pm 0.002
ADV	0.943 \pm 0.002	0.834 \pm 0.007	0.032 \pm 0.001	0.010 \pm 0.001	0.967 \pm 0.001	0.988 \pm 0.001
ORTH	0.967 \pm 0.000	0.898 \pm 0.001	0.014 \pm 0.000	0.017 \pm 0.002	0.986 \pm 0.000	0.982 \pm 0.002
CelebA (Eyeglasses)						
ERM	0.999 \pm 0.000	0.988 \pm 0.001	0.002 \pm 0.000	0.008 \pm 0.003	0.998 \pm 0.000	0.992 \pm 0.003
UNL	0.998 \pm 0.000	0.986 \pm 0.002	0.003 \pm 0.001	0.008 \pm 0.003	0.997 \pm 0.001	0.992 \pm 0.003
ADV	0.998 \pm 0.000	0.981 \pm 0.002	0.003 \pm 0.000	0.012 \pm 0.005	0.997 \pm 0.000	0.988 \pm 0.005
ORTH	0.999 \pm 0.000	0.991 \pm 0.001	0.001 \pm 0.000	0.005 \pm 0.002	0.999 \pm 0.000	0.995 \pm 0.002
CelebA (Young)						
ERM	0.942 \pm 0.000	0.981 \pm 0.000	0.007 \pm 0.001	0.035 \pm 0.001	0.992 \pm 0.002	0.965 \pm 0.001
UNL	0.941 \pm 0.001	0.980 \pm 0.000	0.008 \pm 0.000	0.036 \pm 0.001	0.992 \pm 0.000	0.964 \pm 0.001
ADV	0.820 \pm 0.063	0.932 \pm 0.026	0.018 \pm 0.012	0.110 \pm 0.041	0.974 \pm 0.018	0.884 \pm 0.045
ORTH	0.946 \pm 0.000	0.982 \pm 0.000	0.008 \pm 0.001	0.032 \pm 0.000	0.991 \pm 0.001	0.967 \pm 0.000
CelebA (Attractive)						
ERM	0.918 \pm 0.001	0.923 \pm 0.002	0.005 \pm 0.001	0.166 \pm 0.002	0.995 \pm 0.001	0.825 \pm 0.001
UNL	0.915 \pm 0.000	0.920 \pm 0.000	0.004 \pm 0.003	0.170 \pm 0.001	0.995 \pm 0.003	0.820 \pm 0.001
ADV	0.815 \pm 0.055	0.811 \pm 0.061	0.004 \pm 0.002	0.292 \pm 0.043	0.995 \pm 0.003	0.659 \pm 0.068
ORTH	0.920 \pm 0.001	0.925 \pm 0.002	0.004 \pm 0.001	0.162 \pm 0.002	0.995 \pm 0.001	0.829 \pm 0.001
CelebA (Blond Hair)						
ERM	0.986 \pm 0.000	0.930 \pm 0.001	0.003 \pm 0.001	0.358 \pm 0.004	0.996 \pm 0.001	0.619 \pm 0.004
UNL	0.987 \pm 0.000	0.932 \pm 0.001	0.005 \pm 0.000	0.377 \pm 0.010	0.995 \pm 0.000	0.601 \pm 0.010
ADV	0.973 \pm 0.000	0.877 \pm 0.003	0.024 \pm 0.002	0.492 \pm 0.015	0.975 \pm 0.002	0.457 \pm 0.018
ORTH	0.987 \pm 0.000	0.934 \pm 0.001	0.001 \pm 0.001	0.334 \pm 0.008	0.999 \pm 0.001	0.647 \pm 0.009



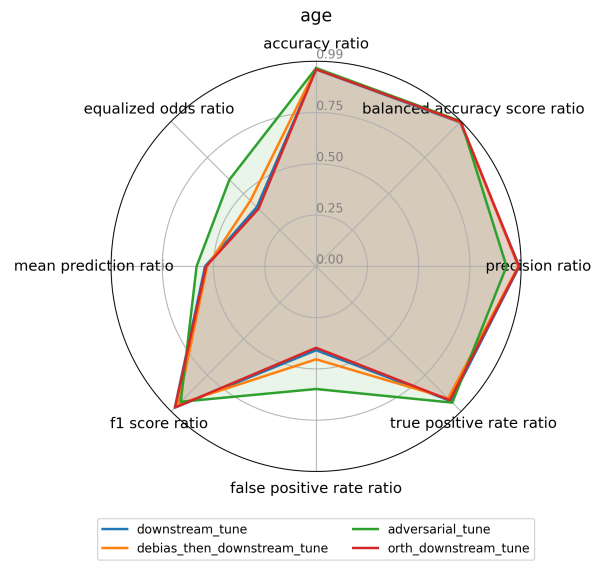
(a) Classifier threshold-independent AUC metrics, where higher values are preferred except for ROC AUC difference and PR AUC difference, for which lower values are preferred.



(b) Classifier threshold-dependent Utility metrics (for a threshold of 0.5), where higher values are preferred except for false positive rate, for which lower values are preferred.

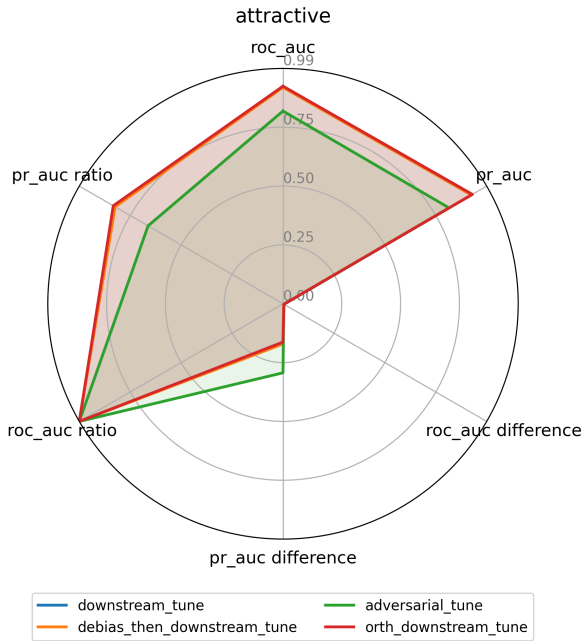


(c) Classifier threshold-dependent fairness difference metrics (for a threshold of 0.5), where lower values are preferred.

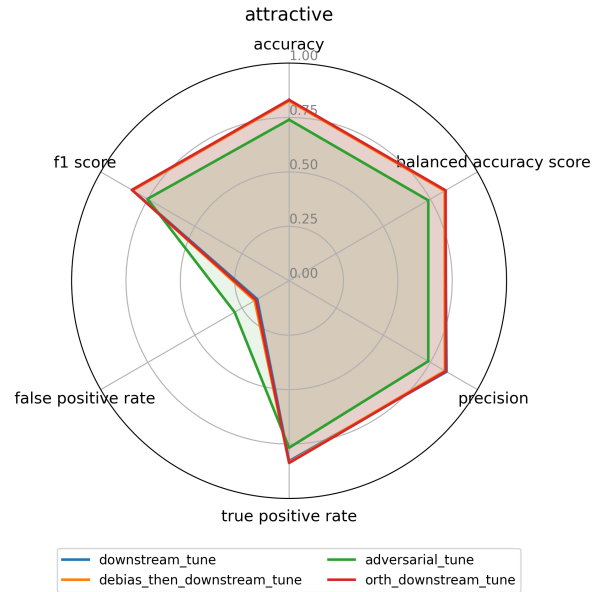


(d) Classifier threshold-dependent fairness ratio metrics (for a threshold of 0.5), where higher values are preferred.

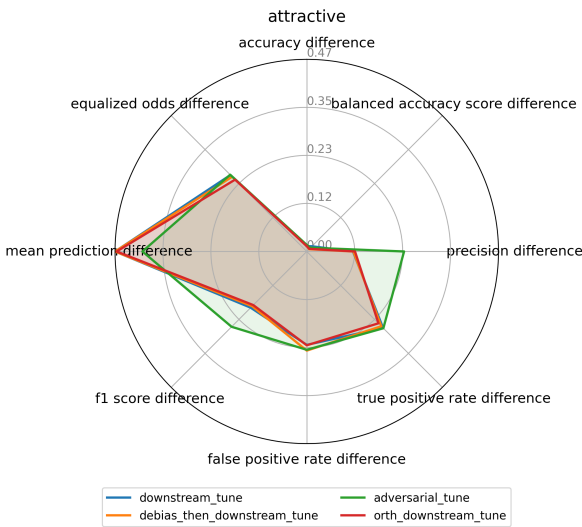
Figure 6. Utility and fairness performance of different fine-tuning strategies on the UTK-Face dataset for the age classification task (with gender as the sensitive attribute). The results are averaged over 3 seeds.



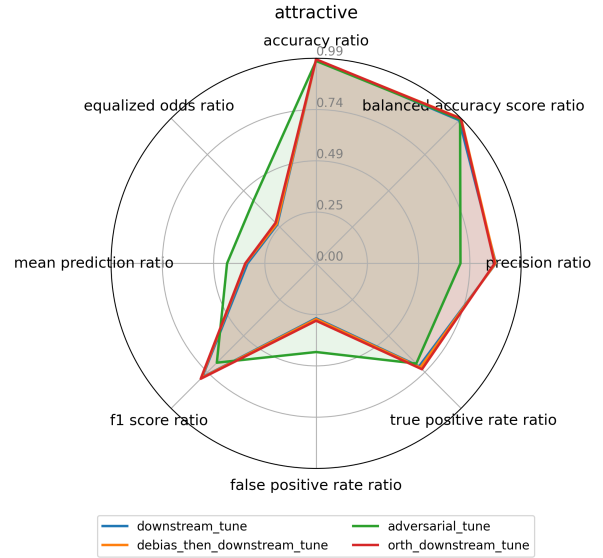
(a) Classifier threshold-independent AUC metrics, where higher values are preferred except for ROC AUC difference and PR AUC difference, for which lower values are preferred.



(b) Classifier threshold-dependent Utility metrics (for a threshold of 0.5), where higher values are preferred except for false positive rate, for which lower values are preferred.

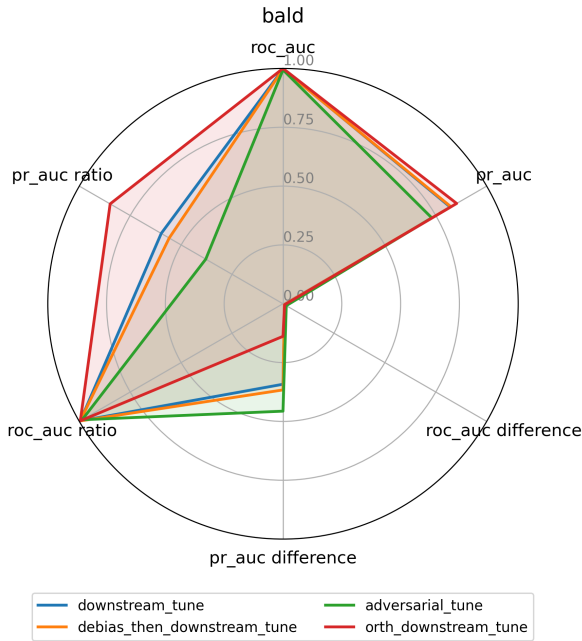


(c) Classifier threshold-dependent fairness difference metrics (for a threshold of 0.5), where lower values are preferred.

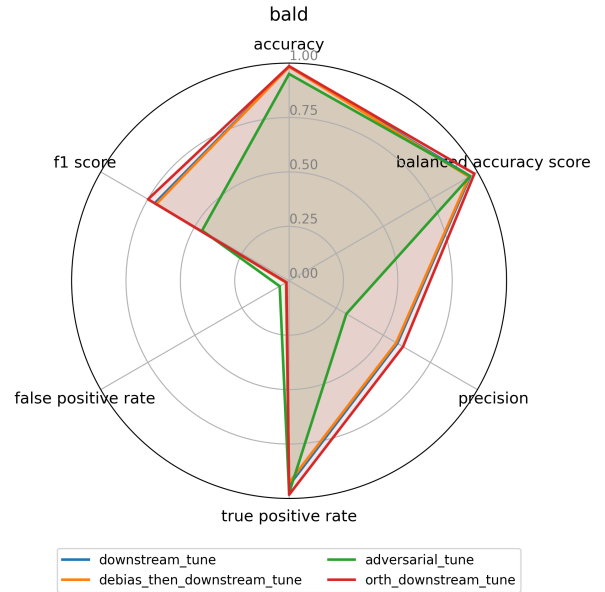


(d) Classifier threshold-dependent fairness ratio metrics (for a threshold of 0.5), where higher values are preferred.

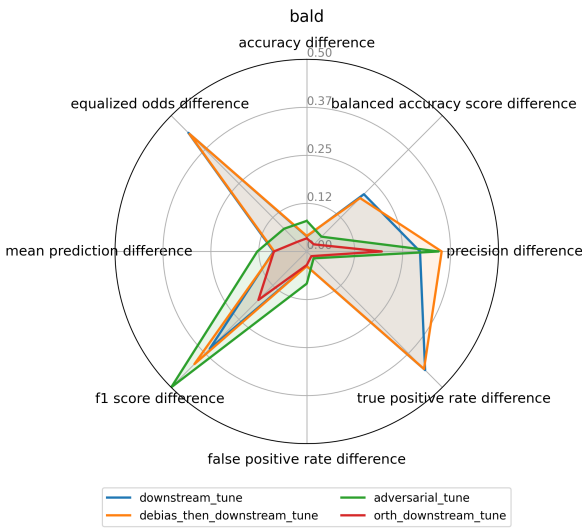
Figure 7. Utility and fairness performance of different fine-tuning strategies on the CelebA dataset for the attractive classification task (with gender as the sensitive attribute). The results are averaged over 3 seeds.



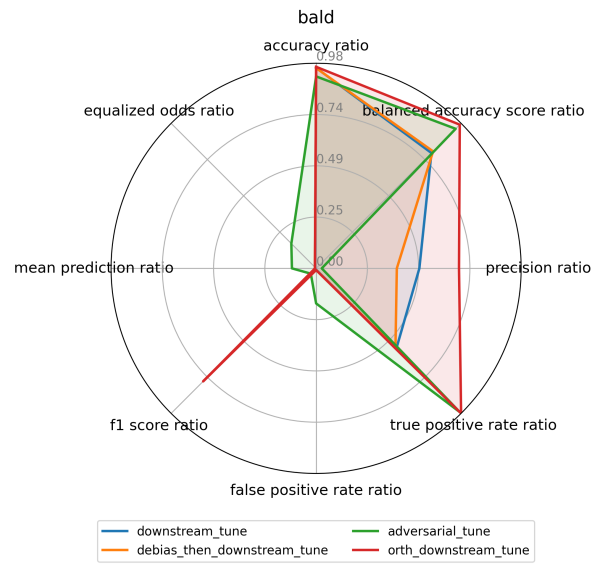
(a) Classifier threshold-independent AUC metrics, where higher values are preferred except for ROC AUC difference and PR AUC difference, for which lower values are preferred.



(b) Classifier threshold-dependent Utility metrics (for a threshold of 0.5), where higher values are preferred except for false positive rate, for which lower values are preferred.

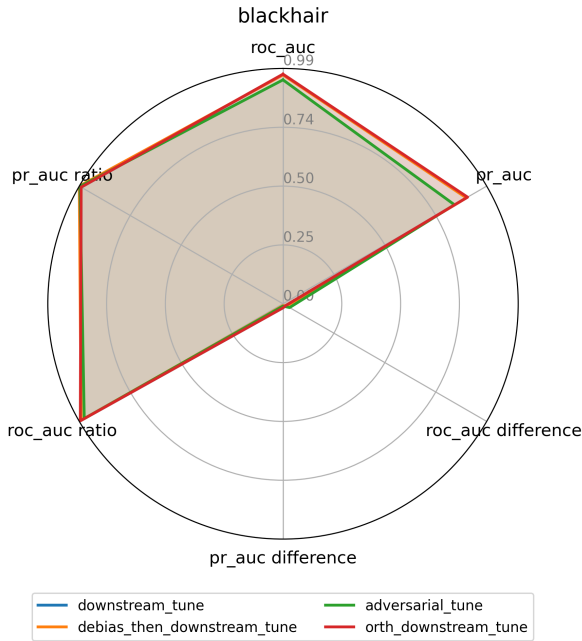


(c) Classifier threshold-dependent fairness difference metrics (for a threshold of 0.5), where lower values are preferred.

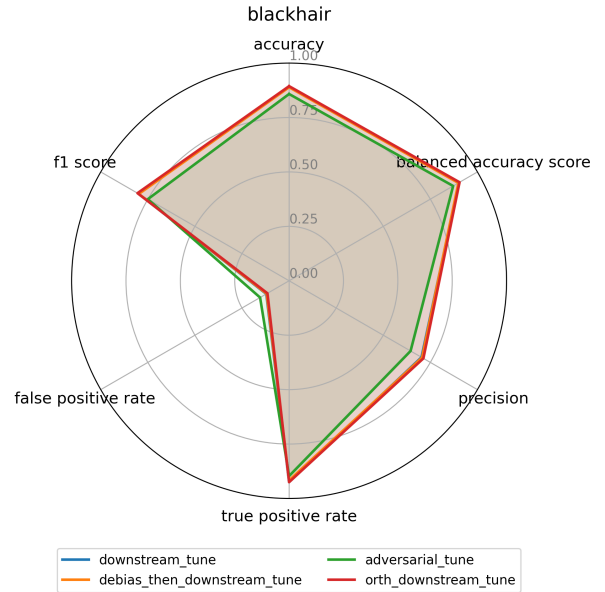


(d) Classifier threshold-dependent fairness ratio metrics (for a threshold of 0.5), where higher values are preferred.

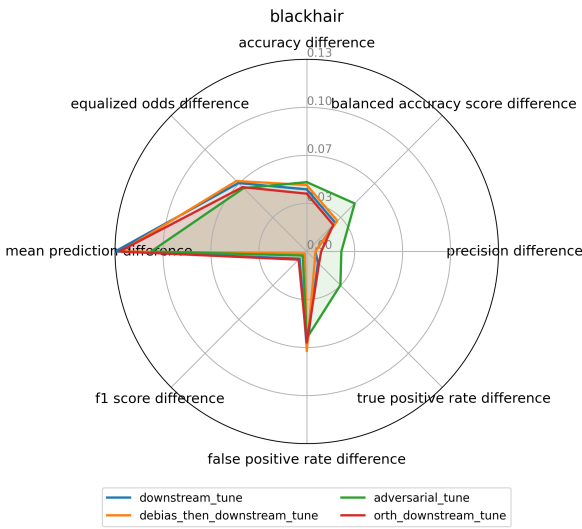
Figure 8. Utility and fairness performance of different fine-tuning strategies on the CelebA dataset for the bald classification task (with gender as the sensitive attribute). The results are averaged over 3 seeds.



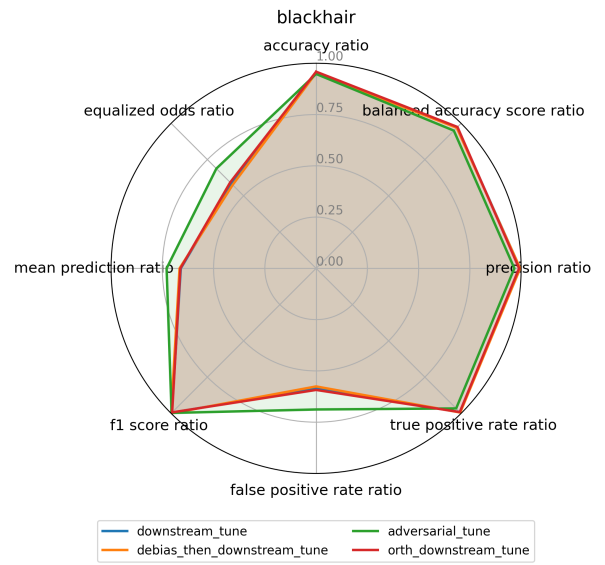
(a) Classifier threshold-independent AUC metrics, where higher values are preferred except for ROC AUC difference and PR AUC difference, for which lower values are preferred.



(b) Classifier threshold-dependent Utility metrics (for a threshold of 0.5), where higher values are preferred except for false positive rate, for which lower values are preferred.

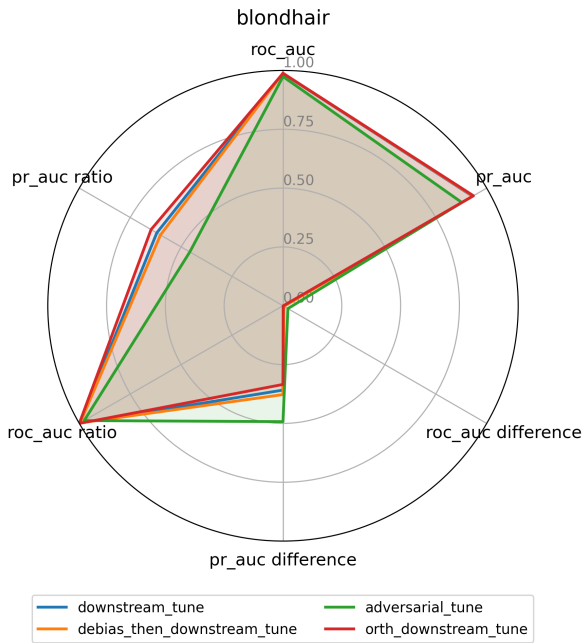


(c) Classifier threshold-dependent fairness difference metrics (for a threshold of 0.5), where lower values are preferred.

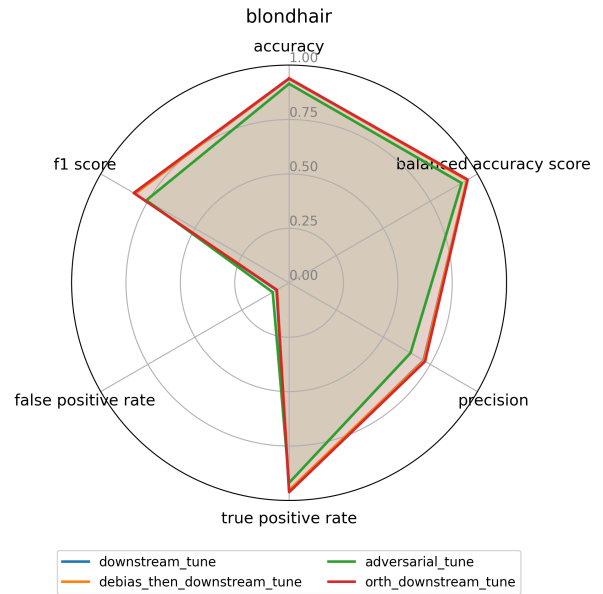


(d) Classifier threshold-dependent fairness ratio metrics (for a threshold of 0.5), where higher values are preferred.

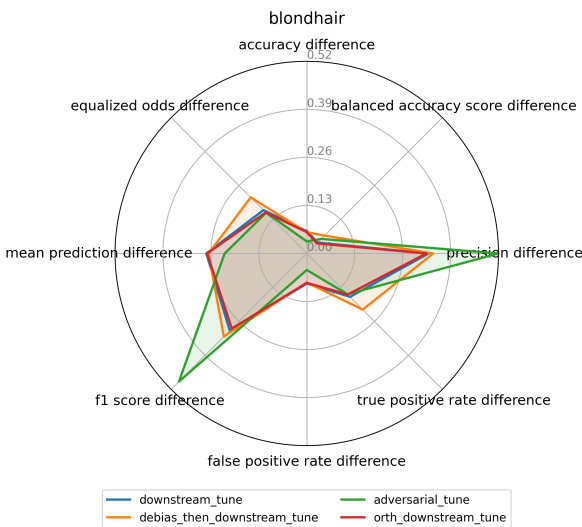
Figure 9. Utility and fairness performance of different fine-tuning strategies on the CelebA dataset for the blackhair classification task (with gender as the sensitive attribute). The results are averaged over 3 seeds.



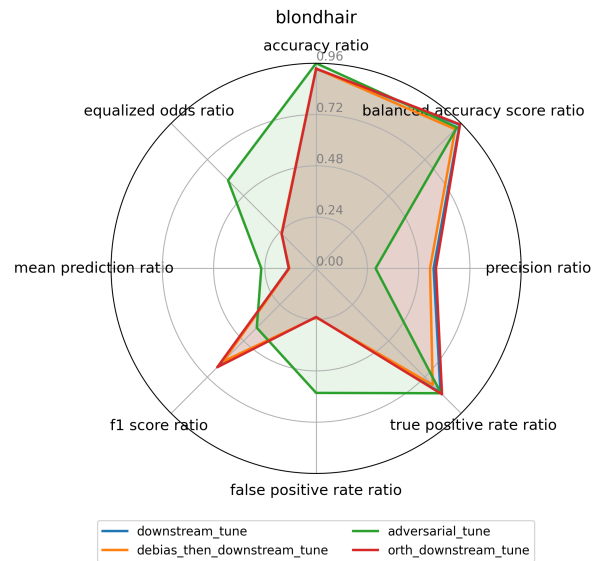
(a) Classifier threshold-independent AUC metrics, where higher values are preferred except for ROC AUC difference and PR AUC difference, for which lower values are preferred.



(b) Classifier threshold-dependent Utility metrics (for a threshold of 0.5), where higher values are preferred except for false positive rate, for which lower values are preferred.

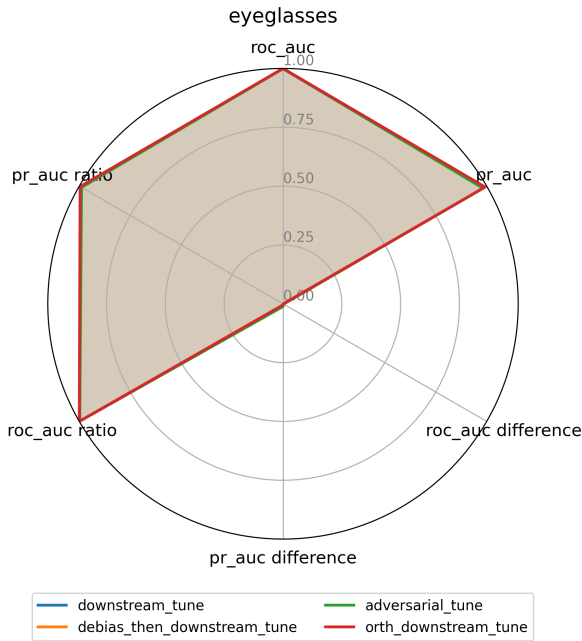


(c) Classifier threshold-dependent fairness difference metrics (for a threshold of 0.5), where lower values are preferred.

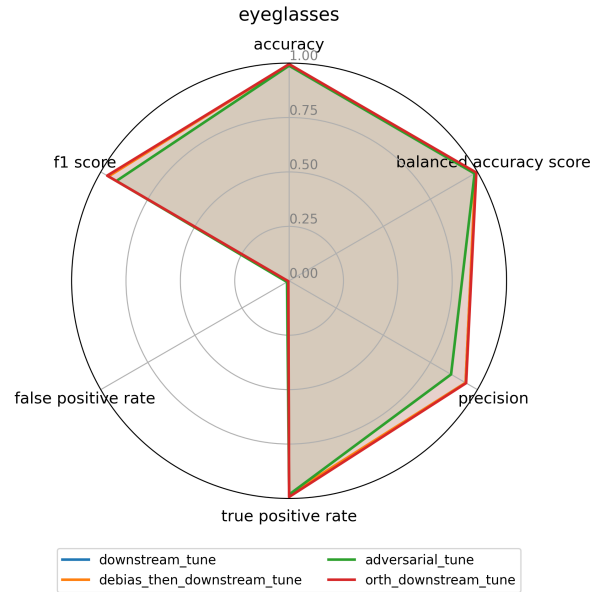


(d) Classifier threshold-dependent fairness ratio metrics (for a threshold of 0.5), where higher values are preferred.

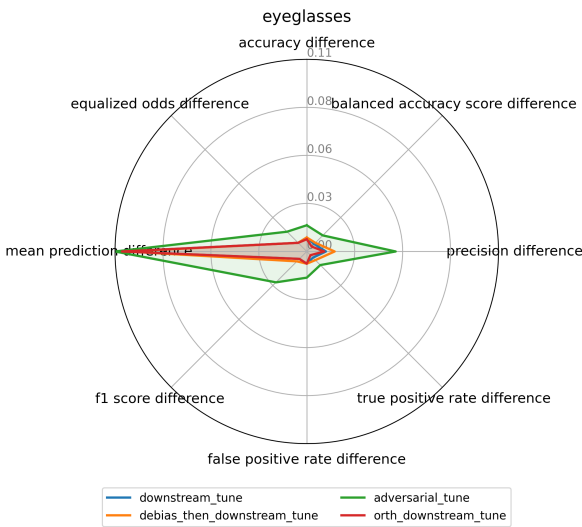
Figure 10. Utility and fairness performance of different fine-tuning strategies on the CelebA dataset for the blondhair classification task (with gender as the sensitive attribute). The results are averaged over 3 seeds.



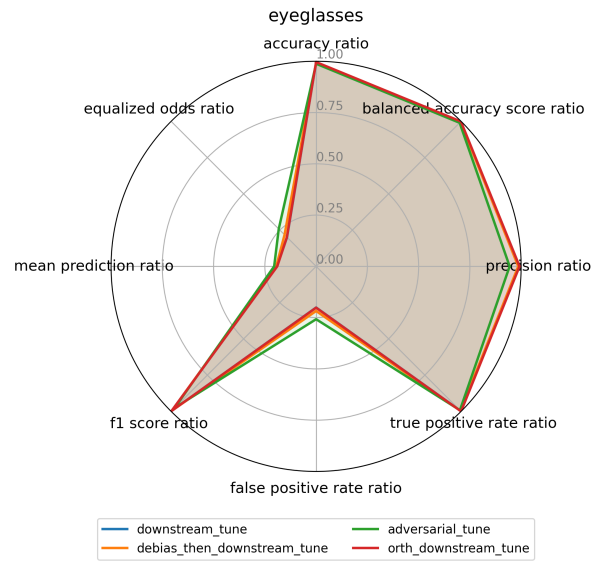
(a) Classifier threshold-independent AUC metrics, where higher values are preferred except for ROC AUC difference and PR AUC difference, for which lower values are preferred.



(b) Classifier threshold-dependent Utility metrics (for a threshold of 0.5), where higher values are preferred except for false positive rate, for which lower values are preferred.

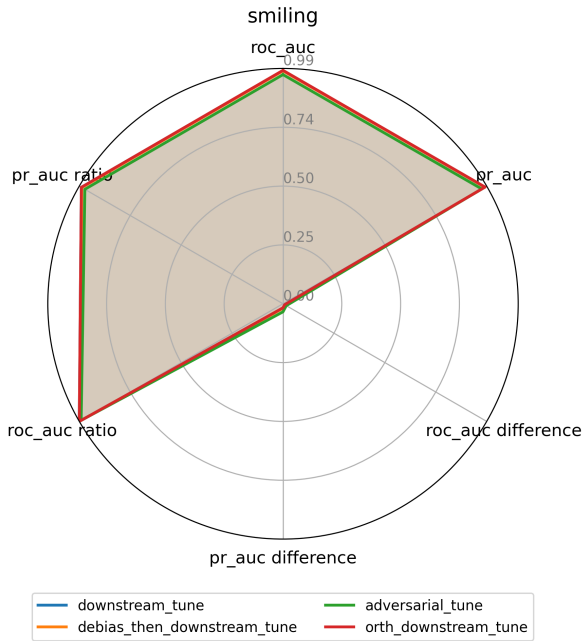


(c) Classifier threshold-dependent fairness difference metrics (for a threshold of 0.5), where lower values are preferred.

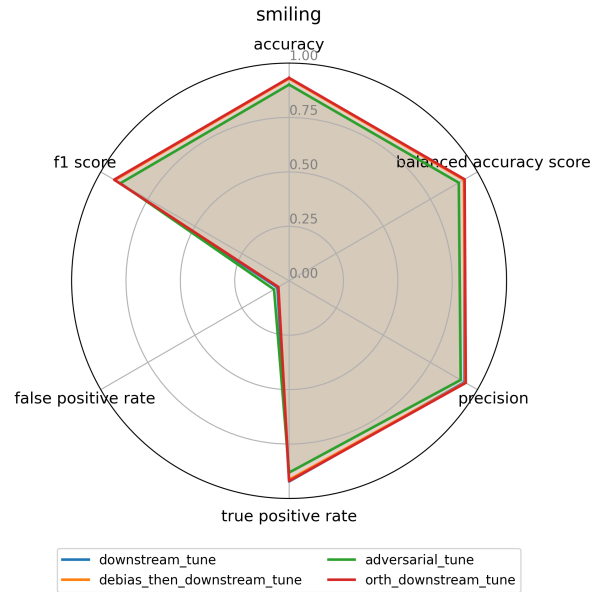


(d) Classifier threshold-dependent fairness ratio metrics (for a threshold of 0.5), where higher values are preferred.

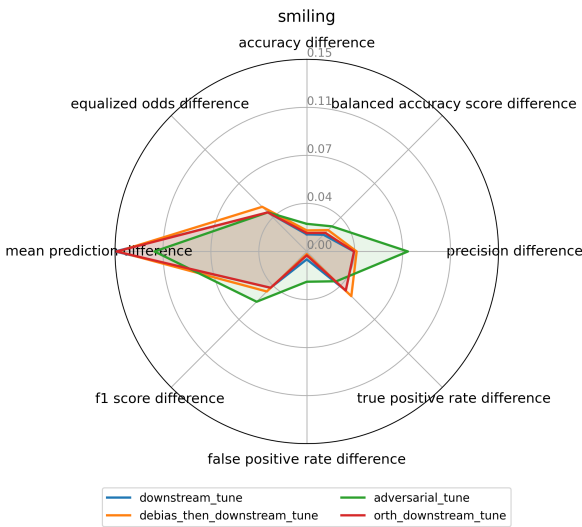
Figure 11. Utility and fairness performance of different fine-tuning strategies on the CelebA dataset for the eyeglasses classification task (with gender as the sensitive attribute). The results are averaged over 3 seeds.



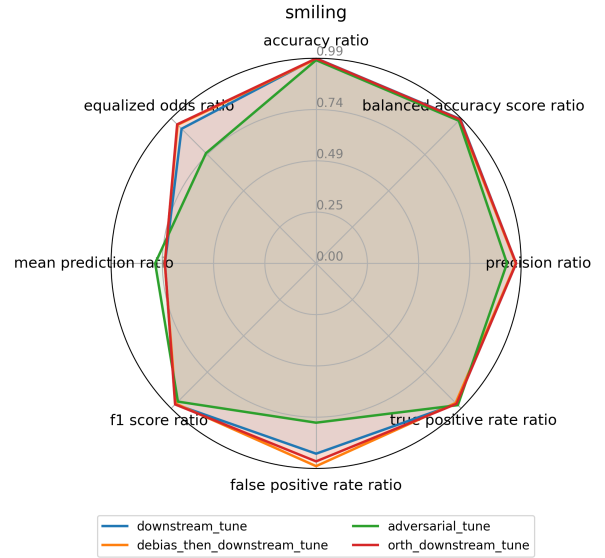
(a) Classifier threshold-independent AUC metrics, where higher values are preferred except for ROC AUC difference and PR AUC difference, for which lower values are preferred.



(b) Classifier threshold-dependent Utility metrics (for a threshold of 0.5), where higher values are preferred except for false positive rate, for which lower values are preferred.

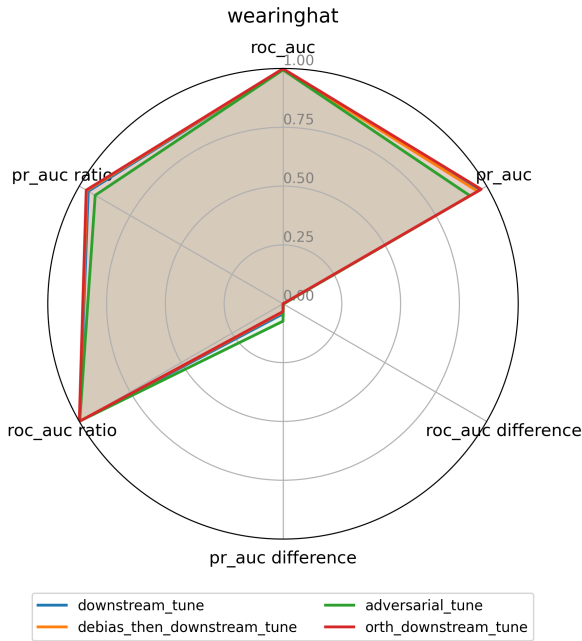


(c) Classifier threshold-dependent fairness difference metrics (for a threshold of 0.5), where lower values are preferred.

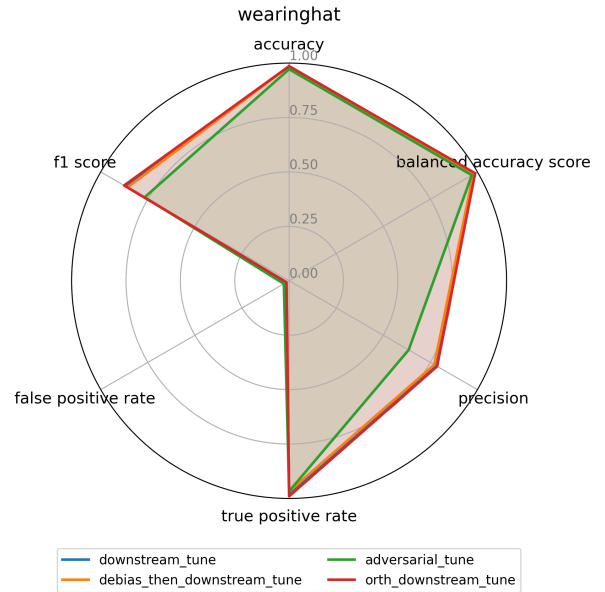


(d) Classifier threshold-dependent fairness ratio metrics (for a threshold of 0.5), where higher values are preferred.

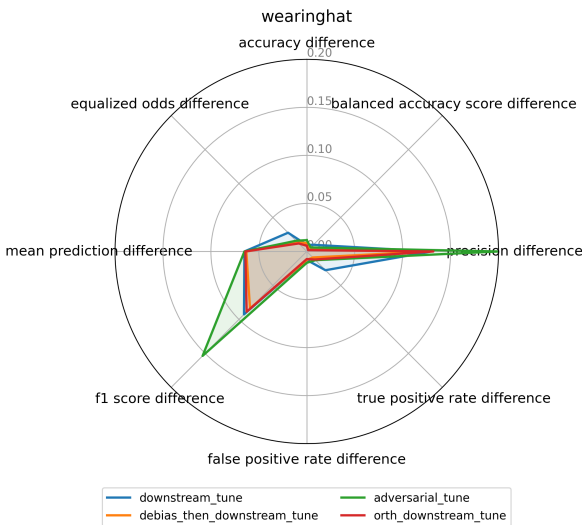
Figure 12. Utility and fairness performance of different fine-tuning strategies on the CelebA dataset for the smiling classification task (with gender as the sensitive attribute). The results are averaged over 3 seeds.



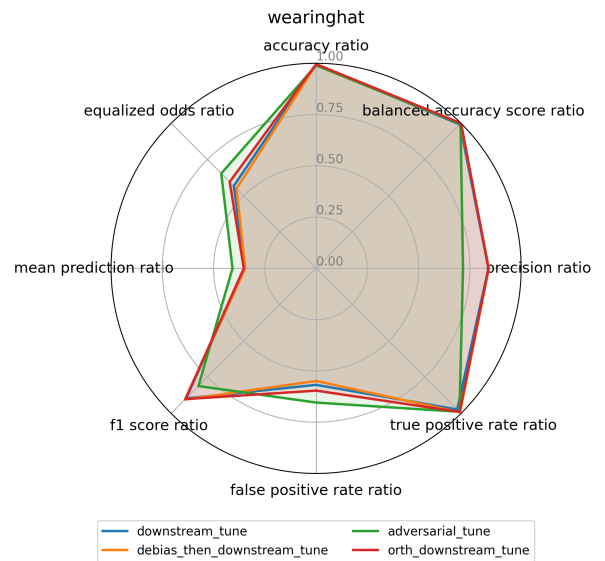
(a) Classifier threshold-independent AUC metrics, where higher values are preferred except for ROC AUC difference and PR AUC difference, for which lower values are preferred.



(b) Classifier threshold-dependent Utility metrics (for a threshold of 0.5), where higher values are preferred except for false positive rate, for which lower values are preferred.

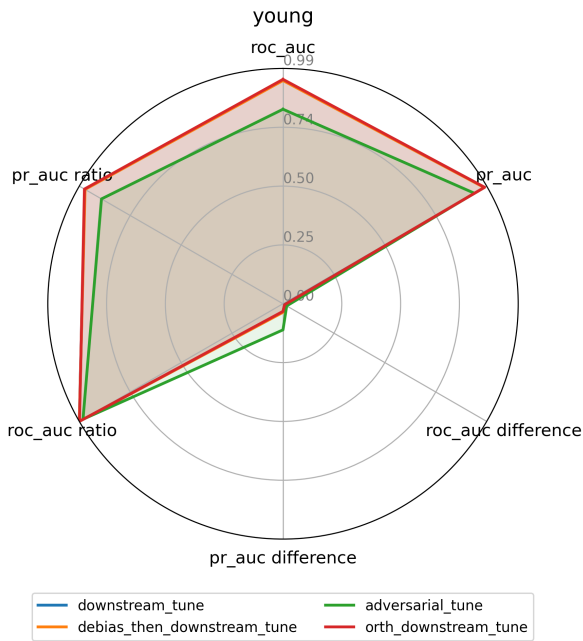


(c) Classifier threshold-dependent fairness difference metrics (for a threshold of 0.5), where lower values are preferred.

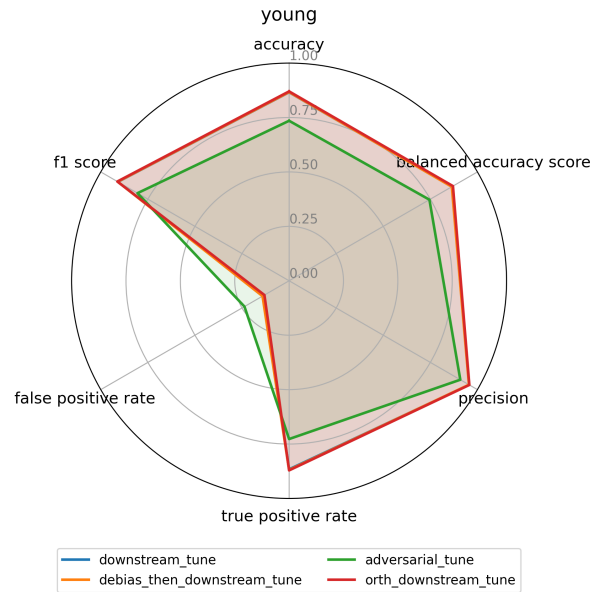


(d) Classifier threshold-dependent fairness ratio metrics (for a threshold of 0.5), where higher values are preferred.

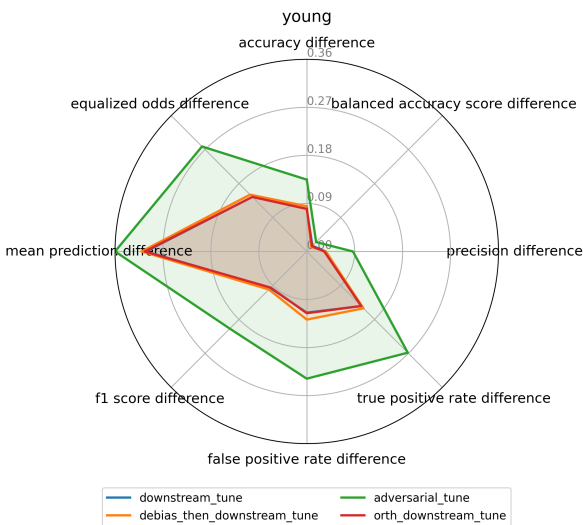
Figure 13. Utility and fairness performance of different fine-tuning strategies on the CelebA dataset for the wearinghat classification task (with gender as the sensitive attribute). The results are averaged over 3 seeds.



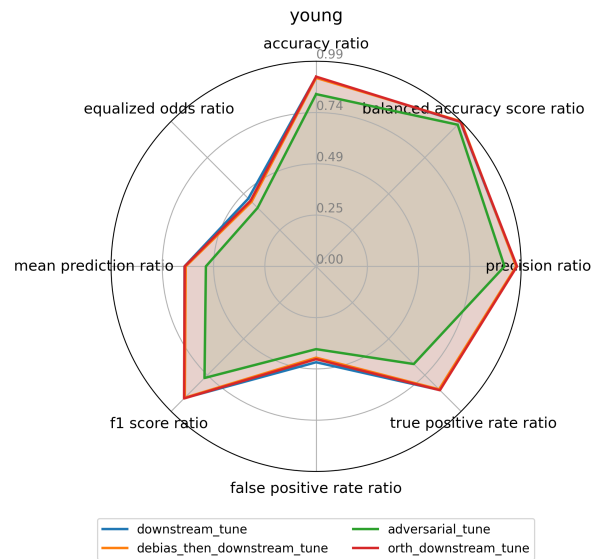
(a) Classifier threshold-independent AUC metrics, where higher values are preferred except for ROC AUC difference and PR AUC difference, for which lower values are preferred.



(b) Classifier threshold-dependent Utility metrics (for a threshold of 0.5), where higher values are preferred except for false positive rate, for which lower values are preferred.



(c) Classifier threshold-dependent fairness difference metrics (for a threshold of 0.5), where lower values are preferred.



(d) Classifier threshold-dependent fairness ratio metrics (for a threshold of 0.5), where higher values are preferred.

Figure 14. Utility and fairness performance of different fine-tuning strategies on the CelebA dataset for the young classification task (with gender as the sensitive attribute). The results are averaged over 3 seeds.